 ISSN 0267-8179. DOI: 10.1002/jqs.3198

JQS Journal of Quaternary Science QRA Quaternary Research Association

Geology, stratigraphy and palaeoenvironmental evolution of the *Stephanorhinus kirchbergensis*-bearing Quaternary palaeolake(s) of Gorzów Wielkopolski (NW Poland, Central Europe)

ARTUR SOBCZYK,[1]* RYSZARD K. BORÓWKA,[2] JANUSZ BADURA,[3] RENATA STACHOWICZ-RYBKA,[4] JULITA TOMKOWIAK,[2] ANNA HRYNOWIECKA,[5] JOANNA SŁAWIŃSKA,[2] MICHAŁ TOMCZAK,[6] MATEUSZ PITURA,[7,1] MARIUSZ LAMENTOWICZ,[8] PIOTR KOŁACZEK,[8] MONIKA KARPIŃSKA-KOŁACZEK,[8] DARIUSZ TARNAWSKI,[9] MARCIN KADEJ,[9] PIOTR MOSKA,[10] MAREK KRĄPIEC,[11] KRZYSZTOF STACHOWICZ,[4] BARTOSZ BIENIEK,[2] KRZYSZTOF SIEDLIK,[2] MAŁGORZATA BĄK,[12] JAN VAN DER MADE,[13] ADAM KOTOWSKI[14] and KRZYSZTOF STEFANIAK[14]

[1]Department of Structural Geology and Geological Mapping, Institute of Geological Sciences, University of Wroclaw, Wrocław, Poland
[2]Geology and Palaeogeography Unit, Faculty of Geosciences, University of Szczecin, Szczecin, Poland
[3]Polish Geological Institute – National Research Institute, Lower Silesia Branch, Wrocław, Poland
[4]W. Szafer Institute of Botany, Polish Academy of Sciences, Kraków, Poland
[5]Polish Geological Institute – National Research Institute, Marine Geology Branch, Gdańsk, Poland
[6]Polish Geological Institute – National Research Institute, Pomeranian Branch, Szczecin, Poland
[7]smartcarto.com, Tomaszów Lubelski, Poland
[8]Department of Biogeography and Palaeoecology, Institute of Geoecology and Geoinformation, Adam Mickiewicz University in Poznań, Poznań, Poland
[9]Department of Invertebrate Biology, Evolution and Conservation, Institute of Environmental Biology, University of Wroclaw, Wrocław, Poland
[10]Division of Radioisotopes, Institute of Physics, Centre for Science and Education, Silesian University of Technology, Gliwice, Poland
[11]AGH University of Science and Technology, Faculty of Geology, Geophysics and Environment Protection, Kraków, Poland
[12]Palaeoceanography Unit, Faculty of Geosciences, University of Szczecin, Szczecin, Poland
[13]Museo Nacional de Ciencias Naturales, Consejo Superior de Investigaciones Científicas, Madrid, Spain
[14]Department of Palaeozoology, Institute of Environmental Biology, University of Wroclaw, Wrocław, Poland

Received 13 January 2019; Revised 17 January 2020; Accepted 13 March 2020

ABSTRACT: The sedimentary succession exposed in the Gorzów Wielkopolski area includes Eemian Interglacial (MIS 5e) or Early Weichselian (MIS 5d–e) deposits. The sedimentary sequence has been the object of intense interdisciplinary study, which has resulted in the identification of at least two palaeolake horizons. Both yielded fossil remains of large mammals, alongside pollen and plant macrofossils. All these proxies have been used to reconstruct the environmental conditions prevailing at the time of deposition, as well as to define the geological context and the biochronological position of the fauna. Optically stimulated luminescence dating of the glaciofluvial layers of the GS3 succession to 123.6 ± 10.1 (below the lower palaeolake) and 72.0 ± 5.2 ka (above the upper palaeolake) indicate that the site formed during the Middle–Late Pleistocene (MIS 6 – MIS 5). Radiocarbon-dating of the lacustrine organic matter revealed a tight cluster of Middle Pleniglacial Period (MIS 3) ages in the range of ~41–32 ka cal BP (Hengelo – Denekamp Interstadials). Holocene organic layers have also been found, with ^{14}C ages within a range of 4330–4280 cal BP (Neolithic). Pollen and plant macrofossil records, together with sedimentological and geochemical data, confirm the dating to the Eemian Interglacial. Copyright © 2020 John Wiley & Sons, Ltd.

KEYWORDS: Eemian Interglacial; OSL dating; palynology and macrofossil analysis; Quaternary stratigraphy; radiocarbon dating

Introduction

A well-preserved, nearly complete skeleton of Merck's rhinoceros *Stephanorhinus kirchbergensis* (Jäger, 1839) has recently been found at an Eemian Interglacial site near Gorzów Wielkopolski, in north-western Poland. The remains were discovered in 2016 during works along the S3 Polish national road. They were located at the southern end of an escarpment along the road. The skeleton was preserved in a succession that had accumulated in a small, shallow kettle palaeolake formed during the Scandinavian ice sheet retreat. The Gorzów deposits belong to at least two limnic cycles: an older one, dating to the Eemian Interglacial (MIS 5e); and an overlying one of Mid-Weichselian (MIS 3) age. The rhinoceros remains were preserved in a gyttja layer of the former unit. Besides the skeletal remains of *S. kirchbergensis*, the site also yielded an isolated left metacarpal bone of fallow deer, *Dama dama* (Linnaeus, 1758), from the basal part of a peat layer that lies over the rhinoceros-bearing gyttja. The rhinoceros skeleton includes the cranium, with full dentition, and almost 120 postcranial bones. The lumbar and caudal part of the spinal column, as well as the left hind limb and a few minor bones, were not preserved. All the bones are exceptionally well preserved; the skull of the rhinoceros suffered diagenetic crushing and damage caused by the roadworks.

*Correspondence: Artur Sobczyk, as above.
E-mail: artur.sobczyk@uwr.edu.pl

In the European Lowland area, Eemian Interglacial and Early Weichselian deposits are usually found south of the limit of maximum extension of the Weichselian (Vistulian) glaciation (Marks *et al.*, 2016), whereas within the post-Weichselian areas they are reported only from boreholes and pits (Fig. 1). Up until now, only a few Eemian Interglacial sites were known in north-western Poland, and palynological and malacological analysis had been performed at only five of them, i.e. Radówek (Urbański and Winter, 2005), Rzecino (Mirosław-Grabowska, 2008; Winter *et al.*, 2008; Niska and Mirosław-Grabowska, 2015), Rusinowo (Stark *et al.*, 1932), Słubice (Skompski, 1980; Alexandrowicz and Alexandrowicz, 2010) and Nakło (Noryśkiewicz, 1978). Further to the west, Eemian deposits have been documented around the municipality of Poznań and the southern region of Wielkopolska (Straszewska and Stupnicka, 1979; Kuszell and Malkiewicz, 1999; Bruj and Roman, 2007). From the German Brandenburg and Mecklenburg regions, sediments of Eemian age have been reported by Eissmann (2002), Brose *et al.* (2006), Hermsdorf and Strahl (2008), Rother *et al.* (2019) and Börner *et al.* (2018). Middle Pleniglacial deposits of the same age as the upper peats horizon from section GS3 (Fig. 1) of Gorzów Wielkopolski occur in brown-coal open-cast mines in the region of Lausitz (Eastern Germany) (see Mol, 1997; Bos *et al.*, 2001). Kozarski *et al.* (1980) found Brørup strata in a brickyard nearby Drezdenko (Stare Kurowo). Only a few Eemian and Early Weichselian mollusc fauna from these sites were described (Skompski, 1980; Alexandrowicz and Alexandrowicz, 2010), whereas no vertebrate remains had ever been found preserved *in situ* until now. Other fossil-bearing localities with remains of large mammals are Imbramowice, near Wrocław (Marciszak *et al.*, 2017), Warsaw (Czyżewska, 1962; Borsuk-Białynicka and Jakubowski, 1972) and Konin (Lorek, 1988), and other similar sites are known from Eastern Germany (Kolfschoten, 2000; Eismann, 2002; Gaudzinski-Windheuser *et al.*, 2014). The nearly complete skeleton of *S. kirchbergensis* (Jäger, 1839) from Gorzów Wielkopolski is therefore a key reference for the analysis of the Central European Eemian/Early

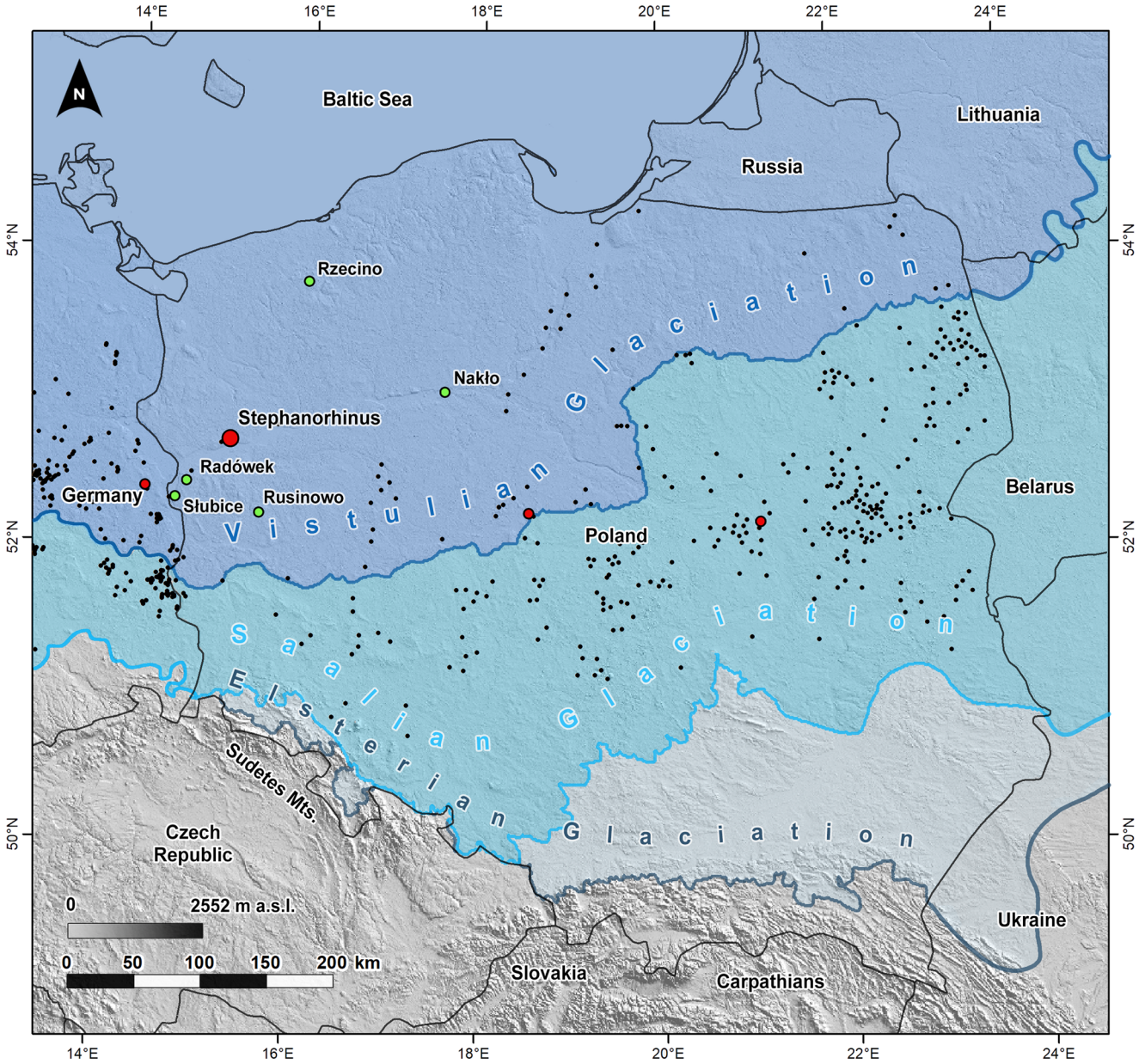

Figure 1. Location of the Eemian Interglacial deposits in Poland and Eastern Germany with indicated Pleistocene Scandinavian Ice Sheet maximum extents. Map explanations: black dots – Eemian Interglacial sites reported in the literature; red dots – sites with fossil bone findings; green dots – sites with palynological and malacological analyses. [Color figure can be viewed at wileyonlinelibrary.com].

Weichselian. This study presents the results of an interdisciplinary research project aimed at performing an in-depth analysis of the rhinoceros from Gorzów Wielkopolski. The paper focuses in particular on the environmental conditions under which the animal lived, as well as on later environmental changes.

Regional setting – study area

The studied area is located in North-western Poland (Fig. 2), ca. 6 km to the west of Gorzów Wielkopolski municipality (51°43′ N; 15°10′ E), along a deep constructional excavation along the S3 national road. The road now cuts through the valley escarpment separating Gorzów Plain, to the north, from the ice-marginal valley of Toruń-Eberswalde to the south. Gorzów Plain is a vast ground morainic plateau intercalated with outwash plain deposits, formed during the maximum extension of the Weichselian glaciation in Western Poland (Germany – Brandenburg phase; Poland – Leszno phase) when, during its climax, the glacial sheets reached the Leszno area, ca. 90 km south of the studied area (Fig. 2A). The ground moraine area is drained to the south by a system of syn- to post-glacial channels, which form a dense network of small erosional, mostly dry, deeply-incised valleys that cut through the morphological crevasse. Gorzów Plain is between 70 and 90 m a.s.l., whereas the base of the Toruń-Eberswalde valley reaches 18–20 m a.s.l. The fossil bones were found at site GS3 (Fig. 2C); they were preserved in a narrow melt-out depression filled with Eemian lacustrine calcareous gyttja (Fig. 3). Two limnic horizons occur in the central GS3 section (Fig. 4A): the lower one is a lacustrine unit of Eemian age, the upper one is of Weichselian (Vistulian) age. The lacustrine succession is capped by a peat bog deposit (Figs 4–6), whereas the upper horizon by glaciofluvial and glacial beds. Section GS1 includes about 11 m of lacustrine deposits that end with fine and medium sand interbedded with silty sand. Section GS2 includes 13.5 m of uniform, unsorted, glaciofluvial sand and gravel. The entire GS2 profile is perhaps an older, presumably Saalian glaciofluvial, sequence, possibly correlated with the basal parts of the GS1 and GS3 successions (Figs 3 and 4).

Methods

Fieldwork and sampling strategy

Geological and geomorphological maps of the Quaternary strata exposed along a road cut near Gorzów Wielkopolski were developed based on a geodetic survey that served to establish a series of cross-sections through which the spatial extent of the extinct lake deposits was defined (Fig. 6). A Leica SR530 dual-frequency GPS RTK receiver supplied with a VRS net correction device was used for the geodetic survey. Geochemical, sedimentological and environmental reconstructions were based on evidence collected from sections of ca. 11 m of the GS1 (Tables S1 and S2 in Supplementary materials) and GS3 (Tables 1 and 2) successions (Figs 2C and 3). Moreover, radiocarbon and OSL dating were performed to define the chronological extent of the exposed sediments (Tables 3 and 4). The GS1, GS2 and GS3 sequences were located on the west side of the S3 road, and section GS4 on the east (Figs 5 and 6). After angle correction, the four sections GS1–GS4 reached total thicknesses of 21.5, 13.5, 22 and 23 m, respectively (Figs 3 and 6). A comparative Racław profile (Fig. 3) was built based on a sketchy description of the section drilled by the cartographic borehole no. 62 (Piotrowski *et al.*, 2010). Detailed sedimentological, geochemical, palynological and plant macrofossil analyses have been performed on the GS1 (Supplementary materials) and GS3 sections (Figs 7–9) in order to define the characteristics of the palaeolake deposits and the environmental context in which they accumulated. Here, we present the results of the detailed analyses for the profile GS3, where the skeleton was found. For the other profiles analysed, readers are referred to the Supplementary materials provided.

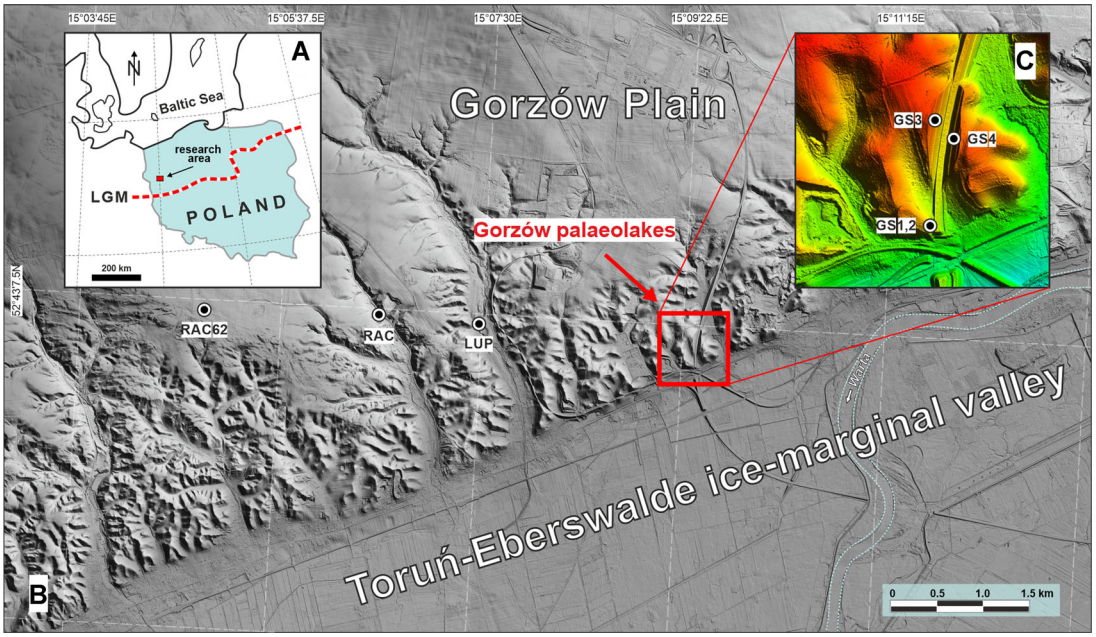

Figure 2. **A** – Location of the research area in Poland at the peak of the Last Glacial Maximum (LGM) during the Late Weichselian (Vistulian) Scandinavian ice sheet advance; **B** – LiDAR-based digital elevation model showing the morphological escarpment separating the Gorzów Lowland (to the north) from west–east-oriented, Toruń-Eberswalde ice-marginal valley. Please note the network of small post-LGM dendritic basins with valleys roughly oriented to the south. Sites of interest mentioned in the text: RAC62 – Borehole Racław 62, which drilled a peat horizon radiocarbon-dated to 34 360 ± 1500 ka cal BP (Lod-820); RAC – borehole with a peat horizon dated to >35 000 BP (Lod-872), LUP – Łupowo site, TL ages from 84.0 ± 12.7 to 79.2 ± 11.9 ka BP; all site locations and data after Piotrowski *et al.* (2010). **C** – Detailed LiDAR representation of the Gorzów Wielkopolski (GS1-GS4) sequences; GS3 is where the bones of rhinoceros, the subject of the present study, were found. [Color figure can be viewed at wileyonlinelibrary.com].

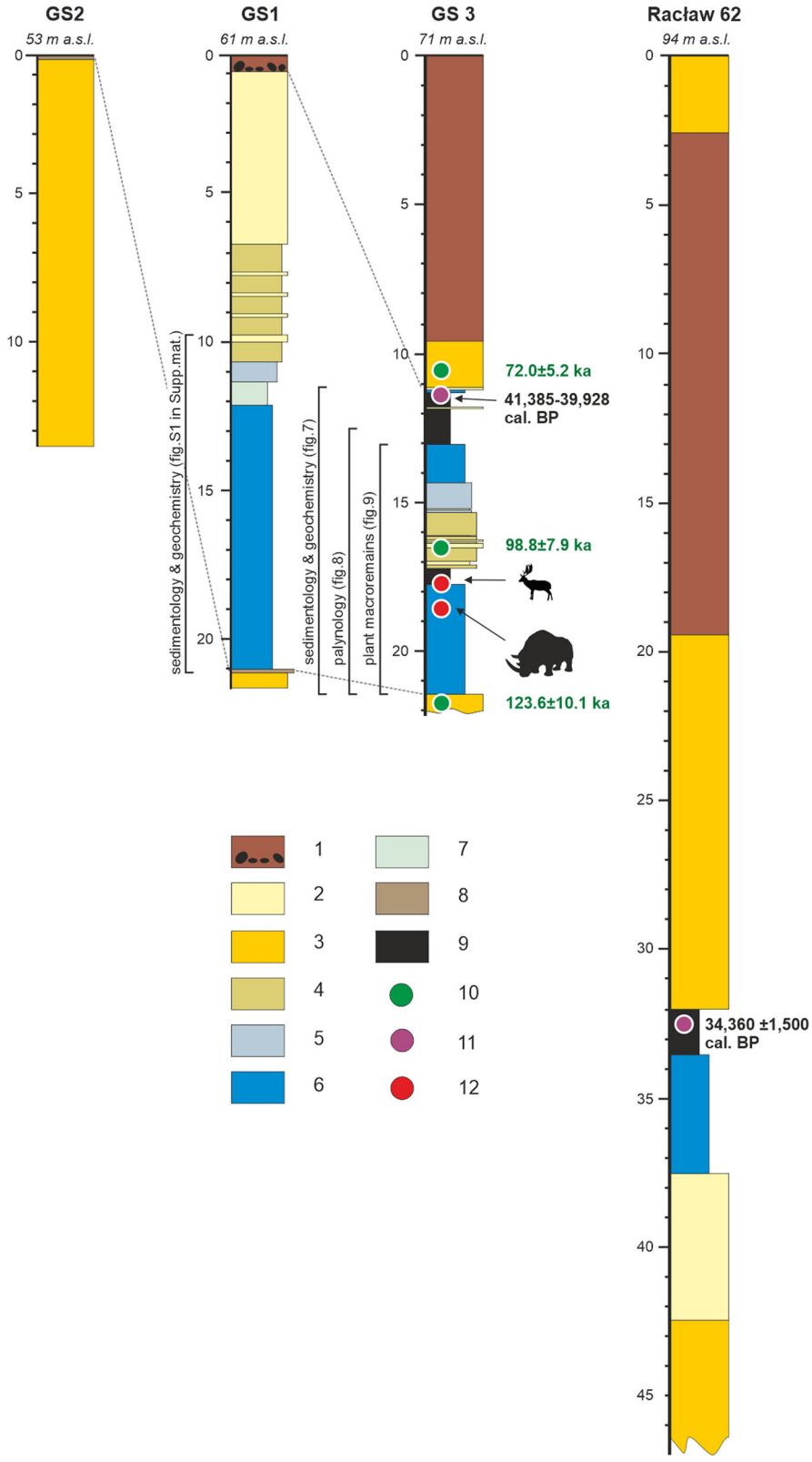

Figure 3 Stratigraphic exposures (in metres) in the Gorzów Wielkopolski area as well as in the Racław 62 borehole (the latter is based on data from Piotrowski *et al.*, 2010). Legend: 1 – Weichselian till with mixed sand and gravel; 2 – fine- and medium-grained sand; 3 – unsorted sand mixed with gravel; 4 – silty sand; 5 – limnic chalk; 6 – gyttja; 7 – sandy silt; 8 – silt; 9 – peat; 10 – OSL age ka BP; 11 – calibrated median radiocarbon age (see Table 5 for details); 12 – bones. [Color figure can be viewed at wileyonlinelibrary.com].

Geochemical and sedimentological analyses

A total of 171 and 181 sediment samples were analysed from the sections GS1 (Supplementary materials) and GS3 (Fig. 7); a constant sampling pace of 6 cm per ca. 11 m was maintained for the lacustrine sediments of the GS1 sequence as well as for the bottom part of the GS3 section. All samples were freeze-dried in a Beta 1-8 LD plus Lyophiliser (Christ). Following homogenisation, some samples were analysed for grain size distribution, using a Mastersizer 3000 laser grain size analyser (Malvern Instruments Ltd). This enabled the determination of the relative percentages of the different grain size fractions, as well as the calculation graphically, according to Folk and Ward (1957), of their major properties: mean grain diameter, standard deviation (SD), skewness and kurtosis. Besides, loss on ignition at 550°C has been calculated on sediment samples of about 2 g dried at 105°C to estimate the percentages of organic and mineral matter content. The organic matter-deprived ash remaining after sediment combustion was treated with 8 ml concentrated nitric acid, 2 ml 10% hydrochloric acid and 2 ml hydrogen peroxide in a Speedwave microwave mineraliser (Berghof). Atomic absorption spectrometry assays

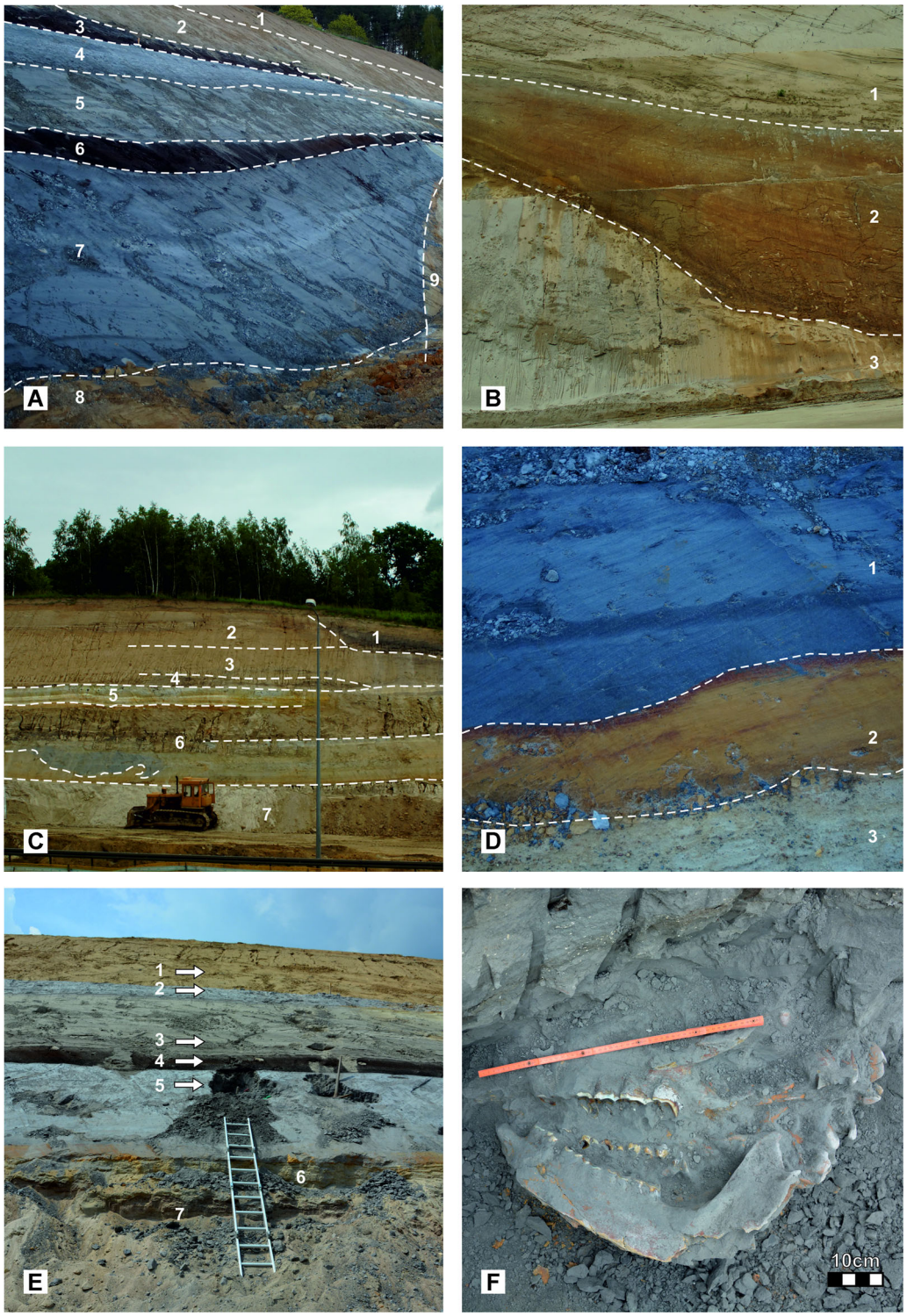

Figure 4. Photographs of sections exposed at the Gorzów Wielkopolski research area. **A** – section GS3: 1 – Weichselian till with mixed sand and gravel; 2 – fine- and medium-grained sand (OSL sample GdTL-2831); 3 – upper Pleni-Weichselian peat; 4 – limnic chalk and gyttja; 5 – sand and silty sand; 6 – lower peat; 7 – limnic chalk and gyttja; 8 – brown gyttja; 9 – Saalian glaciofluvial sand and gravel. **B** – section GS1: 1 – fluvial sand (fan delta); 2 – limnic chalk and gyttja; 3 – Saalian glaciofluvial sand. **C** – section GS4; 1 – organic sand and silt, locally with peat; 2 – mixed glaciofluvial sand and gravelly diamicton; 3 – lacustrine sand, silt and calcareous gyttja; 4 – peat; 5 – lacustrine calcareous gyttja; 6 – fine- and medium-grained sand; 7 – unsorted glaciofluvial sand and gravel. **D** – basal part of sequence GS3: 1 – grey limnic chalk and gyttja; 2 – brown gyttja; 3 – Saalian glaciofluvial sand and gravel. **E** – rhinoceros and deer bone-bearing section: 1 – Weichselian till with mixed sand and gravel; 2 – limnic chalk and gyttja; 3 – sand and silty sand; 4 – peat; 5 – grey limnic chalk and gyttja, showing the site where the bone remains were retrieved; 6 – brown gyttja; 7 – Saalian glaciofluvial sands. **F** – section GS3; the nearly complete skull of *Stephanorhinus kirchbergensis*; a malacological horizon can be recognised just above the skull. [Color figure can be viewed at wileyonlinelibrary.com].

of the solutions obtained, to reveal their content of Na, K, Ca, Mg, Fe, Mn, Cu and Zn, were conducted using an AAS SOLAAR 969 spectrometer (Unicam). Results of the geochemical analyses performed are also presented as geochemical indexes which provide the following information:

- changes in oxidation-reduction conditions – Fe/Mn (Mackereth, 1966; Boyle, 2001; Naeher *et al.*, 2013),
- changes of intensity in chemical and mechanical denudation processes – Na/K, Ca/Mg (Borówka, 1992; Rychel *et al.*, 2014; Pawłowski *et al.*, 2016; Kittel *et al.*, 2016; Mendyk *et al.*, 2016),

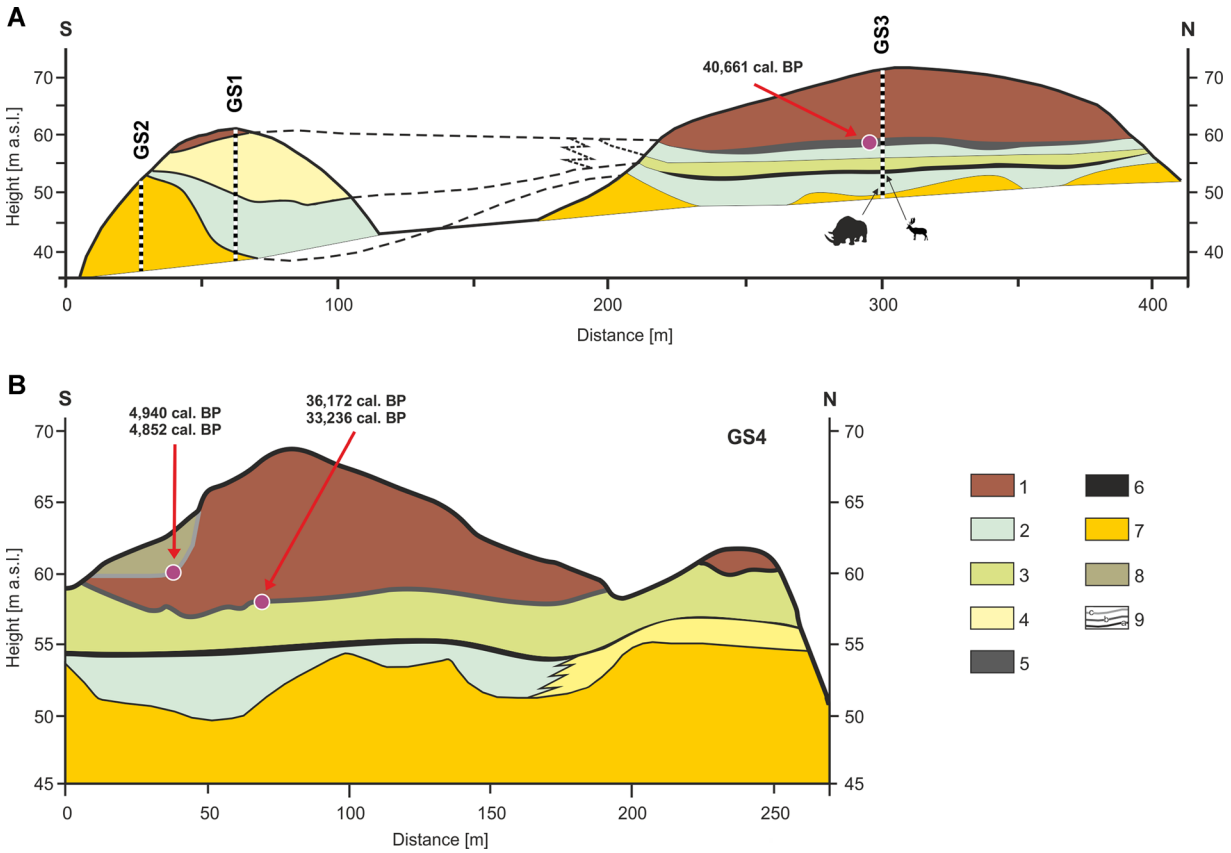

Figure 5. Eastern (A) and western (B) geological cross-sections of the site, projected on a north–south plane. Section GS3 showing where bones were found, as well as section GS4; arrows indicate sampling spots and relative ^{14}C calibrated median radiocarbon ages (see Table 3). Legend: 1 – mixed glaciofluvial sand and gravelly diamicton; 2 – lacustrine lower unit (calcareous gyttja); 3 – lacustrine upper unit (sand, silt and calcareous gyttja); 4 – fine- and medium-grained sand; 5 – limnic chalk; 6 – peat; 7 – unsorted glaciofluvial sand and gravel; 8 – organic sand and silt; 9 – peat: (a) lower, (b) middle and (c) upper horizon. [Color figure can be viewed at wileyonlinelibrary.com].

- changes of intensity in erosional processes – Na+K + Mg/Ca (Ławacz *et al.*, 1978; Kittel *et al.*, 2016; Pawłowski *et al.*, 2016; Karasiewicz, 2019).

The air-dry sediment samples were also used to determine the percentage contributions of total carbon, total nitrogen and total sulphur, using a VARIOMAX CNS analyser (Elementar). All the lithological and geochemical analyses were carried out at the laboratory of the Geology and Palaeography Unit of the University of Szczecin. The data were subjected to statistical treatment, primarily with Microsoft Office Excel software as well as with PAST Palaeontological Statistics (Hammer *et al.*, 2001) to identify geochemical horizons using the stratigraphically constrained cluster analysis of Ward's method. The grain size data were stored and processed using GRADISTAT software (Blott and Pye, 2001), and the C2 programme (Juggins, 2007) was used to visualise the results of laboratory analyses.

Bone remains

The teeth of the rhinoceros were measured according to van der Made (2010) and Shpansky (2016), and the postcranial bones following Gromova (1935, 1960), Guérin (1980) and van der Made (2010); von den Driesch (1976), Di Stefano (1996), Lister (1996) were used for the measurement and identification of the metacarpal bone of fallow deer.

Pollen and plant macroremains

Thirty-five samples for pollen analysis were collected from a depth of 10.26 to 1.38 m (from bottom to top) of section GS3 (Fig. 8). The samples were acetolysed according to Erdtman's method (1960). Before acetolysis, a tablet containing *Lycopodium* spores per 1 cm^3 was added to each sample as a quantitative indicator (Stockmar, 1971; Berglund and Ralska-Jasiewiczowa, 1986). Pollen spectra were counted on two slides from a surface area of 20 × 20 mm routinely up to a total of ca. 500 grains. Thirty-eight samples, each of 150 ml of sediment, were collected for plant macroremains analysis from a depth of 10.26–2.10 m of section GS3, at intervals of 10–40 cm (the same adopted for the pollen sampling). The samples were macerated with 10% KOH, boiled to a pulp, and wet-sieved using a ϕ 0.2 mm mesh sieve. The concentrated sieved residue was then sorted under a stereoscopic microscope. Plant remains that could be identified were selected and placed in a mixture of glycerine, water and ethyl alcohol (1:1:1) with the addition of thymol. Macrofossils were identified with the use of keys, atlases (e.g. Cappers *et al.*, 2006; Velichkevich and Zastawniak, 2006, 2008) and literature data, as well as using a reference collection of present-day seeds and fruits and collections of fossil flora housed in the Palaeobotanical Museum of the W. Szafer Institute of Botany at the Polish Academy of Sciences, Kraków. Qualitative and quantitative results of the plant macrofossil analysis are presented in a diagram (Fig. 9) plotted with POLPAL software for Windows (Nalepka and Walanus, 2003). Local Macrofossil Assemblage Zones (L MAZ) were distinguished in the diagram of macroscopic plant remains from section GS3; they were numbered and labelled, from base to top, GS3-M1 to GS3-M8.

Geochronological data

Three optically stimulated luminescence datings (OSL; Fig. 10, Table 4) and five radiocarbon ^{14}C datings (Table 3) were

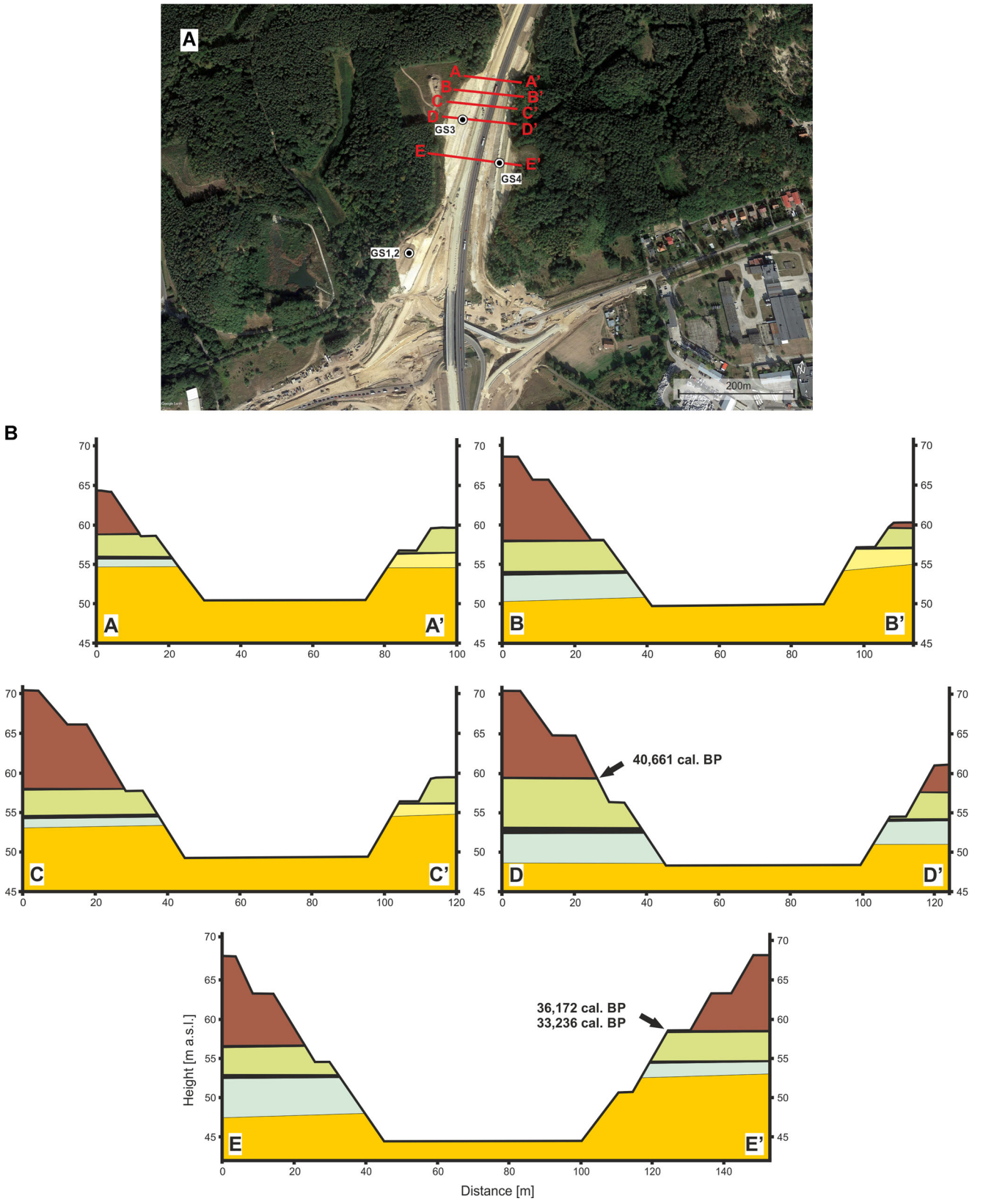

Figure 6. (A) Map showing the location of detailed geological cross-sections (B) based on a geodetic survey conducted in the Gorzów Wielkopolski area, along the S3 national road excavation. Location of the GS1–GS4 sections and the calibrated median radiocarbon-dated levels. For the legend of the lithostratigraphic units see Fig. 5. [Color figure can be viewed at wileyonlinelibrary.com].

performed for representative stratigraphic horizons of sections GS3 and GS4 (Figs 3–5). OSL measurements were made on samples of glaciofluvial sand collected from three different levels of section GS3 by the Department of Radioisotopes of the Silesian University of Technology, according to standard procedures (for details see Aitken, 1998; Galbraith *et al.*, 1999; Murray and Wintle, 2000; Guérin *et al.*, 2011). The samples were collected with steel tubes: (1) 21.8 m b.s.l. at the bottom of the lower palaeolake section; (2) 16.5 m b.s.l., from a ca. 2 m thick interlayer between the two lacustrine successions; and (3) 10.5 m b.s.l., ca. 0.5 m at the top of the upper (second) palaeolake section. High resolution gamma spectrometry using an HPGe detector (Canberra) was carried out in order to determine the content of U, Th and K in the samples. Dose

Table 1. Lithology of the GS3 profile (lower part).

Depth (m)	Height (m a.s.l.)	Lithology
0.00–1.80	59.61–57.81	Dark grey sandy and silty peat with intercalations of organic silt
1.80–1.93	57.81–57.68	Black peat
1.93–4.18	57.68–55.43	Light grey limnic chalk
4.18–6.30	55.43–53.31	Light brown silt and sandy silt
6.30–6.94	53.31–52.67	Black peat
6.94–10.93	52.67–48.68	Grey limnic chalk

rates were calculated using the conversion factors of Guerin *et al.* (2011). For all luminescence samples, the internal alpha-dose rate of the etched and heavy-liquid separated quartz was considered (Jacobs, 2004). To determine this effect μDose system (Tudyka *et al.*, 2018) was used for finely milled subsample. Using an alpha-efficiency value of 0.04 (Rees-Jones, 1995), internal alpha-dose rates were calculated. Estimated water content is lowest for the youngest sample because the humidity of older samples was affected by the palaeolake, which was in this place in the past. For the beta dose-rate, the cosmic ray dose-rate to the site was determined according to Prescott and Stephan (1982). Sand-sized grains of quartz (90–200 μm in diameter) were extracted from the sample using standard purification procedures (e.g. Aitken, 1998). All OSL measurements were made using an automated Risø TL/OSL DA-20 reader for multi-grain aliquots, each of ca. 1 mg. The stimulation light source was a blue (470 ± 30 nm) light-emitting diode array (LED) delivering 50 mW/cm^2 at the sample (Bøtter-Jensen *et al.* 2000). Detection was through 7.5 mm of Hoya U-340 filter. Equivalent doses were determined using the single-aliquot regenerative-dose protocol (Murray and Wintle, 2000). Final OSL ages were calculated using the Central Age Model (Galbraith *et al.* 1999) and presented on radial plots. Plant macrofossils and peat of the upper palaeolake succession of GS3 and two peat layers of section GS4 have been radiocarbon-dated: the upper layer of GS4 is located in a hollow on the top of glacial till and a lower one just below the base of glacial succession (Figs 3–5; Table 3).

Results

Lithology and geochemistry

The ca. 11 m of section GS3 analysed for this study includes gyttja, limnic chalk, silty sand and peat layers (Figs 4A and 7; Table 1). There is a dominance of silt, mixed with minor amounts of fine and very fine sand. Sand characterises in particular the middle part of the section, at around 4.5–6.0 m; they lie over 60 cm of black peat (Fig. 4A). Mean grain sizes (Mz) range around 5–6 ϕ units; sorting (SD) constantly reaches 1.5 ϕ (Fig. 8A). Skewness changes remarkably only at the bottom and in the central part of the section, ranging from −0.2 to 0.5 phi. Kurtosis is persistently one phi all but at the very bottom (10.5 m) of the sequence. Geochemical analyses revealed significantly high Ca content (200–320 mg/g) in the limnic facies and elevated levels of organic matter at 0–2 m and 6.5–7.0 m (Table 2). The highest values of the total carbon, nitrogen and sulphur indexes occur at a transition from the organic mud to peats. Ca/Mg and Na/K indexes reach the highest values in the gyttja/limnic chalk horizons, whereas Fe/Mn increase significantly for the peat horizon. The Na +K + Mg/Ca ratio reaches maximum values at 0–2 m and 4.5–6.5 m, and is negligible elsewhere. Six geochemical zones have been identified in section GS3 (Fig. 7).

Palaeobotanical analysis

The frequency of pollen was from high to very high, indicating a strongly vegetated landscape. The results of the pollen analysis of section GS3 are presented graphically in a percentage pollen diagram (Fig. 8) plotted using POLPAL software for Windows (Nalepka and Walanus, 2003); 12 L PAZ could be distinguished, based on the samples GS3-1 to GS3-12. The lowermost part of the GS3 section (10.14 m) is opened with *Betula*, *Juniperus* and *Pinus* pollen assemblages (Fig. 8) deposited on the top of the Saalian glaciofluvial sequence. On the other hand, there are numerous steppe communities with Poaceae and *Artemisia* as well as tundras with *Betula nana* and Cyperaceae. During this period, at the level of GS3-M1 L MAZ (Fig. 9) the local vegetation was initially dominated by Characeae, which appeared in the lake. At the bottom of the reservoir they occurred in communities that preferred clear water rich in calcium carbonate, which encrusted their thalli. As a result, the sediment was supplemented with calcium carbonate.

The beginning of the Eemian Interglacial was marked by the development of bright and open birch-pine forests (GS3-2 *Betula-Pinus*), with an admixture of *Ulmus* in more humid places (GS3-3 *Pinus-Betula-Ulmus*; Fig. 8). Herbaceous vegetation was becoming increasingly rare at the time. Then forests evolved into the *Quercetum mixtum* communities (GS3-4 *Quercus-Fraxinus-Ulmus*; 9.90 m), in which *Quercus* became dominant and *Pinus* was abundant. There was a

Table 2. Matrix of correlation (r) between the contents of organic matter and selected geochemical elements for the limnic chalk from the Gorzów GS3-3 profile (**bold** – lower chalk; regular – upper chalk).

	LOI	Total C	Total N	Total S	TOC	Na	K	Ca	Mg	Fe	Mn	Cu	Zn
LOI	1	**0.74**	**0.81**	**0.81**	**0.88**	0.06	0.30	**−0.74**	−0.34	**0.63**	0.45	**0.60**	**0.68**
Total C	0.48	1	**0.81**	0.42	**0.84**	0.14	0.07	−0.36	−0.11	0.22	0.09	0.34	0.37
Total N	**0.68**	**0.79**	1	**0.66**	**0.80**	−0.03	0.20	−0.44	−0.08	**0.61**	**0.56**	0.47	**0.55**
Total S	**0.63**	0.45	**0.80**	1	**0.76**	0.01	0.44	**0.83**	−0.45	**0.90**	**0.62**	**0.74**	**0.85**
TOC	**0.71**	**0.82**	**0.97**	**0.78**	1	0.27	0.46	**−0.68**	−0.21	**0.60**	−0.28	**0.66**	**0.74**
Na	−0.12	**−0.59**	**−0.65**	−0.41	**−0.64**	1	**0.66**	−0.18	0.19	0.08	−0.39	0.30	0.27
K	−0.29	**−0.62**	−0.48	−0.28	**−0.52**	0.28	1	**−0.53**	0.22	**0.56**	0.08	**0.63**	**0.68**
Ca	0.24	**0.87**	**0.54**	0.22	**0.57**	**−0.52**	**−0.51**	1	0.34	**−0.69**	−0.27	**−0.68**	**−0.75**
Mg	0.05	**0.54**	0.16	−0.01	0.23	−0.19	**−0.61**	**0.53**	1	−0.24	−0.28	−0.31	−0.36
Fe	−0.20	**−0.81**	**−0.50**	−0.14	**−0.53**	0.46	**0.64**	**−0.83**	**−0.66**	1	**0.69**	**0.71**	**0.80**
Mn	−0.29	−0.49	−0.41	−0.24	−0.40	0.33	0.07	−0.39	−0.18	0.19	1	0.36	0.39
Cu	0.07	0.11	0.03	0.05	0.08	−0.19	0.32	0.25	0.02	−0.11	−0.10	1	**0.79**
Zn	−0.27	**−0.85**	**−0.58**	−0.26	**−0.60**	0.40	**0.73**	**−0.78**	**−0.66**	**0.85**	0.25	0.04	1

Table 3. Results of radiocarbon dating, ages calibrated using the OxCal INTCAL13 approach (Reimer *et al.*, 2013). Explanations for abbreviations: m a.s.l. (metres above sea level); m b.s.l. (metres below surface level); [a] – $d^{13}C$ values measured with AMS on graphite extracted from samples; N/A – data not available due to not enough material suitable for AMS measurements.

Sample number	Laboratory code	Sampling altitude (m a.s.l.)/depth (m b.s.l.)	Dated material and geological context	Conventional age (yr BP)	Cal 1 sigma years BP (95%)	Cal yr BP (median prob.)	$\delta^{13}C$ (‰VPDB)
GS3-1	Beta-493676	58.7/12.0	Macrofossils Upper paleolake peat, just below OSL sample	36 010 ± 330	41 385–39 928	40 661	N/A
GS4-2	Poz-97161	58.1/9.9	Upper paleolake peat	32 200 ± 500	37 710–35 032	36 172	−30.7[a]
GS4-3	Poz-97162	58.0/10.0	Upper paleolake peat	29 060 ± 310	33 906–32 402	33 236	−30.6[a]
GS4-4	MKL-3527	59.9/8.1	Peat on the glacial till top	4280 ± 110	5280–5163 (7.1%) 5135–5105 (1.5%) 5077–4526 (86.9%)	4852	−27.2 ± 0.3
GS4-5	MKL-3526	60.0/8.0	Peat on the glacial till top	4330 ± 120	5303–4780 (79.6%) 4770–4580 (15.8%)	4940	−26.3 ± 0.3

marked small increase in the participation of herbaceous plants. In the level of GS3-M2 L MAZ (Fig. 9), the local presence of several tree species growing close to the shore of the lake is confirmed by the fruit and fruit scales of *Betula* sect. *Albae*, fruits of *Alnus glutinosa* as well as by the remains of *Pinus sylvestris*. At that time there were already communities similar to contemporary reed bed with *Typha* sp. in the lake. *Najas marina* and *Nuphar lutea* appeared at this time, which indicates that the water in the reservoir had grown progressively warmer.

The appearance of *Corylus* in association with *Quercus* (GS3-5 *Corylus-Quercus-Alnus*) and, successively, also with *Tilia cordata* (GS3-6 *Corylus-Tilia-Alnus*) indicates a further improvement of climatic conditions. *Alnus* was also important at this time; it was accompanied by *Ulmus* and *Fraxinus*, which indicates the development of riparian communities. In addition to the macroremains of birch, pine and alder, the level of GS3-M3 L MAZ also provided remains of *Tilia platyphyllos*, which indicates the local presence of this other species of lime in the vicinity of the reservoir. The communities of largely rooted macrohydrophytes were dominated by floating species, among which are *Najas marina*, *Nuphar lutea*, *Brasenia* sp., and *Trapa natans*.

The climatic optimum of the Eemian Interglacial was characterised by the development of oak-hornbeam forests, including *Carpinus*, *Corylus*, *Quercus* and *Tilia cordata*, as well as of riparian forests, mainly represented by *Alnus* (GS3-7 *Carpinus-Corylus-Alnus*; Fig. 8). The upper part of the level of GS3-M3 L MAZ (Fig. 9) provided fruit of *Carpinus betulus* and nuts of *Corylus avellana*, while in the lake, alongside other species characteristic of the climate optimum, such as *Brasenia* sp. and *Trapa natans*, *Najas marina* was ever more present. The level of GS3-M4 L MAZ, which is also included in a time period of the climatic optimum, was characterised by an increased presence of rush vegetation, including *Cladium mariscus*, *Typha* sp. and *Schoenoplectus lacustris*.

The very significant increase in the proportion of peat vegetation such as *Eleocharis palustris* and *Carax pseudocyperus*, versus the other zones observed for the depth interval most likely results from gradual shallowing of the basin and intensive overgrowth of its shores.

The disappearance of *Carpinus*, which was gradually replaced by pinewoods including *Picea*, *Abies* and *Pinus sylvestris*, indicates a climatic and soil deterioration (GS3-8 *Picea-Abies-Carpinus*). As a consequence, *Pinus* completely dominated the surrounding landscape (GS3-9 *Pinus*; Fig. 8), which is tantamount to the approaching end of the Eemian Interglacial. Interestingly, observed short-time *Abies* presence (~7.00–6.50 m) and its abrupt cessation preceding fine-grained material sedimentation (Figs 7 and 8) might indicate shifting toward more arid conditions reported for the Northern Hemisphere between 122 and 118 ka (Sirocko *et al.*, 2005). Also, the results of the analysis of macroremains from level GS3-M5 L MAZ (Fig. 9) indicate that the reservoir was progressively infilling with sediment. The diaspores of aquatic plants have disappeared and peat vegetation, with numerous mosses and sedges, begins to dominate. A dwarf birch appeared again in the environment, and this indicates the deterioration of climatic conditions, which is another argument for the regional-scale progressive aridisation. Results of palaeobotanical analysis stays in general agreement with an age of glaciofluvial sequence dated with OSL to 98.8 ± 7.9 ka, which closes from above the GS3-M5 macrofossil zone.

The cooling of the climate at the beginning of Weichselian glaciation is confirmed by the dwindling and significant withdrawal of woody communities. A characteristic element of this time was *Calluna vulgaris*, together with numerous herbaceous plants (GS3-10 *Calluna vulgaris*-NAP-*Pinus*); *Juniperus* and *Pinus* also appeared in this period (Fig. 8). The reservoir became shallow and was dominated by *Sphagnum*, which resulted in the formation of a peat bog. Humid areas were inhabited by tundra communities, typified by the presence of *Betula nana*. The depletion of species, the drop in frequency

Table 4. Laboratory codes of investigated GS3 profile, samples depth (m b.s.l. = meters below surface level), specific activities of natural radionuclides, dose rates, calculated mean ages for all investigated fractions using the CAM model.

Lab. Code	Sampling depth (m b.s.l.)	U (Bq/kg)	Th (Bq/kg)	K (Bq/kg)	Internal alpha-dose rate (Gy/ka)	Dose rate (Gy/ka)	Water content (%)	Number of measured aliquots	Equivalent dose (Gy)	OSL central age (ka)
GdTL-2831	10.5	4.4 ± 0.1	6.0 ± 0.2	192 ± 6	0.050 ± 0.02	0.85 ± 0.05	12 ± 3	19	61 ± 2	72.0 ± 5.2
GdTL-2830	16.5	4.8 ± 0.1	4.7 ± 0.1	206 ± 6	0.040 ± 0.02	0.82 ± 0.06	15 ± 5	58	81 ± 2	98.8 ± 7.9
GdTL-2829	21.8	8.4 ± 0.2	6.7 ± 0.2	257 ± 7	0.047 ± 0.02	1.03 ± 0.08	18 ± 5	47	127 ± 3	123.6 ± 10.1

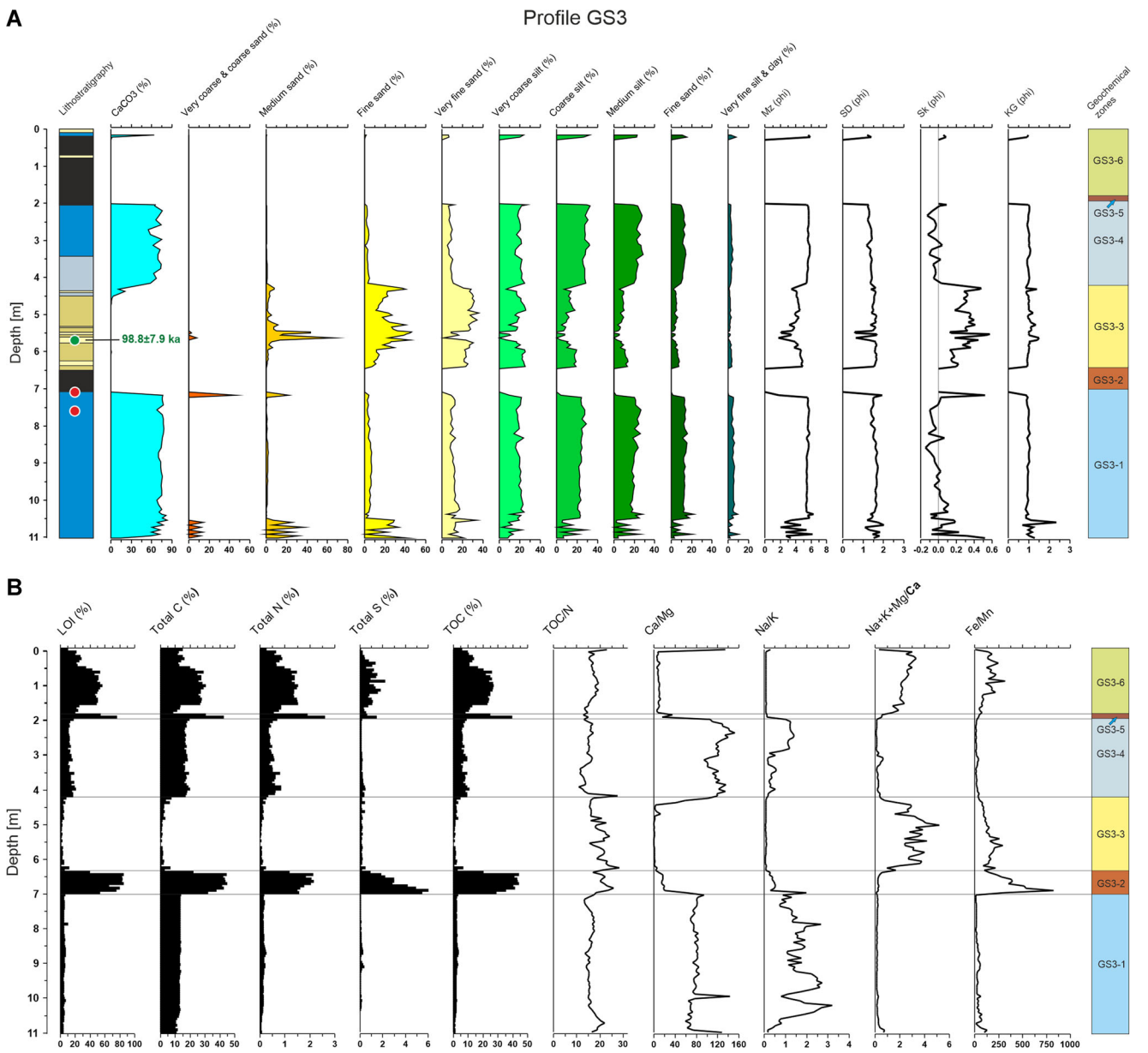

Figure 7. Results of the sedimentological and geochemical analyses of section GS3 and measured OSL age. See text for explanations. [Color figure can be viewed at wileyonlinelibrary.com].

of plant macroremains in all the ecological groups present in the GS3-M6 L MAZ level and the highest amounts of sclerotia of *Cenococcum geophilum* in the entire sequence indicate that robust processes of re-sedimentation were underway along the banks of the reservoir, which explains the numerous occurrences of thermophilic tree pollen (Fig. 9).

Further cooling led to the withdrawal of *Pinus*, as well as to the spread of a pioneering and heliotropic birch tree in a landscape dominated by herbaceous communities (GS3-11 *Betula*-NAP). A relatively stable, but cold, climate led to the development of rare pine and birch forests mixed with herbaceous vegetation (lower part of GS3-12 *Pinus-Betula*, Fig. 8). The numerous macroremains of dwarf birch (*Betula nana*) at the level GS3-M7 L MAZ indicate an increase in the amount of shrub tundra-type vegetation surrounded by a lake. The aquatic vegetation of *Potamogeton filiformis* is also indicative of cold climatic conditions. The results of the plant macroremains analysis in the last determined level GS3-M8 L MAZ correlate with those of the palynological analysis performed in the upper part of the level GS3-12 L PAZ, where variable values of *Pinus* and *Betula* indicate fluctuations in unstable climatic conditions, but with a slight warming trend. The transition of from *Najas marina* and *Najas flexilis* aquatic plant assemblages at this level may indicate a slight short-term improvement of climatic conditions, while Characeae oospores denote a new deepening of the palaeolake (Fig. 9).

Bone remains

Some bones of *S. kirchbergensis* were found still preserved in anatomical connection; others were disarticulated and displaced (Fig. 4F). The bone surfaces are virtually unabraded and unaffected by weathering. They show no evidence of hunting or butchering by humans, nor of carnivore ravaging. The teeth are heavily worn, which indicates that the individual reached relatively old age. Based on the size of its long bones, the individual stood about 182 cm at the withers, which makes it one of the largest known representatives of the species. Its size probably discouraged predators from attacking it.

The fallow deer from Gorzów Wielkopolski is the earliest known representative of *D. dama* in the Polish fossil record. Up to this moment, the only known fossil remains of fallow

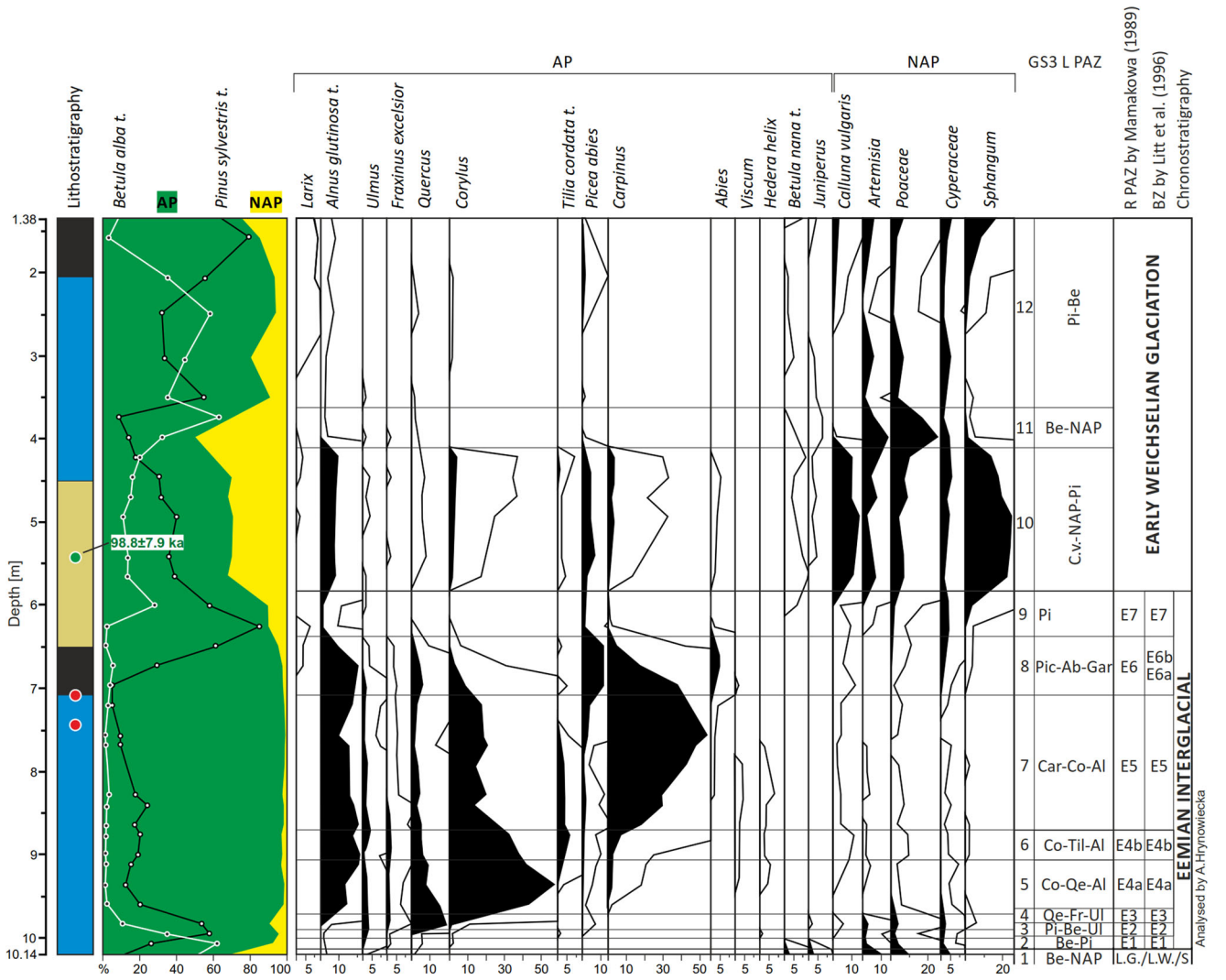

Figure 8. Simplified pollen diagram of section GS3 and measured OSL age. Acronyms GS3 L PAZ are explained in the text. Legend: R PAZ – Regional Pollen Assemblage Zone, BZ – Biostratigraphic Zone; L.G. – Late Glacial; L.W. – Late Wartanian; S – Saalian. [Color figure can be viewed at wileyonlinelibrary.com].

deer were from the Lower Pleistocene (MIS 58-40) deposits of Żabia Cave, which are assigned to *Dama* cf. *farnetensis* (Stefaniak, 2015). Other finds of fallow deer, mentioned in earlier literature (Kowalski, 1959; Czyżewska, 1989) are reported from historical sites and are now lost to record. The extant *D. dama* was introduced in Poland in the early Middle Ages as a park animal (Kowalski, 1959; Czyżewska, 1989). This discovery adds to the list of Polish Interglacial fauna and corresponds to findings reported from Western European Eemian sites (e.g. Björck *et al.*, 2000).

Geochronological data

Combined OSL and radiocarbon dating of the GS3 sequence (Fig. 3) revealed a period ranging from the Late Saalian (ca. 130 ka) to the Mid-Holocene (ca. 5 ka). OSL results were obtained on quartz grains collected from basal, central and upper inorganic horizons under, between and over, respectively, the lower and upper palaeolake deposits.

Equivalent dose distributions (Berger, 2010) are presented in Fig. 10, obtained overdispersions are in the range from 7% to 16%, which is why the Central Age Model (CAM) (Galbraith *et al.*, 1999) was used for final De calculations. The OSL central ages are between 123.6 ± 10.1 and 72.0 ± 5.2 ka (Table 4; Fig. 10) and regularly grow younger toward the top of the sequence. The upper palaeolake, macrofossil-bearing, organic-rich, black peat horizon lying just above the OSL-dated GdTL-2831 sample (72.0 ± 5.2 ka) was radiocarbon-dated.

This sample gave an age of 40 661 cal yr BP (Table 3). Radiocarbon dating of four samples collected from the middle and upper peat horizons (Fig. 5B) of section GS4 yielded two groups of ages: the oldest (36 172–33 236 cal yr BP) were recorded in the middle peat and can be referred to the Mid-Pleniglacial (MIS3) phase; the youngest Mid-Holocene ages (4940–4852 cal yr BP) were recorded in the peat located on top of the glacial till. The OSL dating defined the minimum age of glaciofluvial sequence that deposited before the formation of the first Eemian palaeolake, whereas the radiocarbon ages place clearer chronological limits on the history of the evolution of the younger palaeolake.

Discussion

The results of lithological and geochemical studies of the sediments filling the analysed sedimentary basin, as well as the radiocarbon and OSL ages and the results of the palaeobotanical analysis, delineate distinct stages of evolution of the palaeolakes (see Table 5 for the summary). The local stratigraphic succession starts to deposit at ca. 170–180 ka during the Late Saalian (Wartanian) glaciation in a glacial/

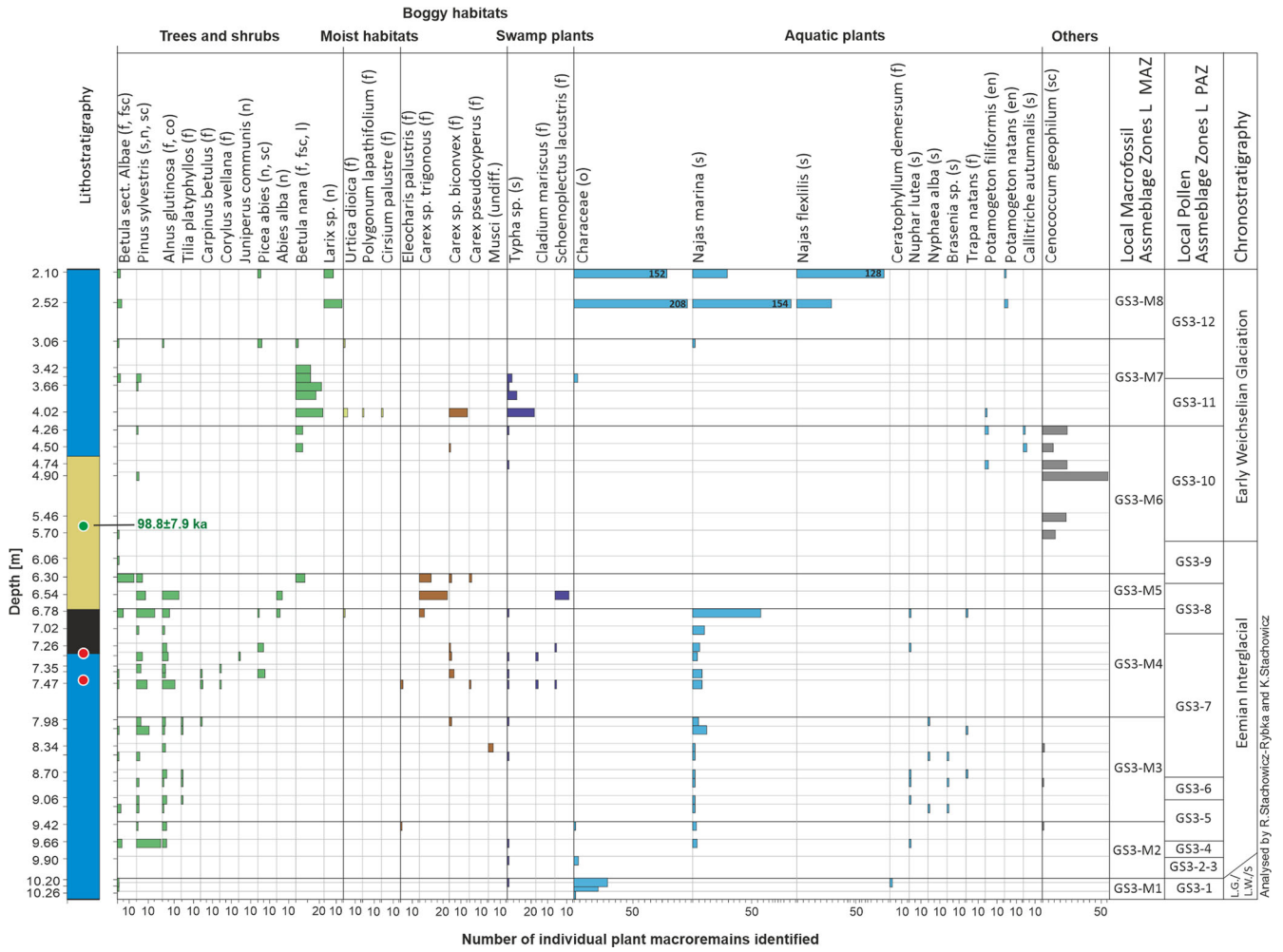

Figure 9. Summary diagram of macrofossils from section GS3 and measured OSL age. Legend of abbreviations: f – fruit, fsc – fruit scales, sc – scales, s – seed, en – endocarp, n – needle, co – cone, sk – sclerocia, l – leaf. The scale below the diagram shows the quantitative results of the plant macroremains. Legend: L MAZ – Local Macrofossils Assemblage Zone, L.G. – Late Glacial; L.W. – Late Wartanian (Late Saalian); S – Saalian. [Color figure can be viewed at wileyonlinelibrary.com].

glaciofluvial environment, as indicated by the oldest OSL-dated quartz grains, sometime before the formation of the lower palaeolake (Fig. 11). The lake began to develop in the Early Eemian coinciding with climate warming; carbonate gyttja accumulated, together with a fairly significant amount of allochthonous minerals. In the coastal zone, sandy material reached the basin; a quite significant proportion of it was found in the lower part of section GS1 (Fig. 4B). During this phase, the lake was supplied not only by calcium carbonate-rich groundwater but also, to a large extent, by surface waters, which brought in allochthonous materials (Fig. S1 in Supplementary materials). The high proportion of manganese and iron oxides and hydroxides in the sediments of this phase indicates that oxidising conditions prevailed both in the coastal zone and off the lakeshore. High concentrations of manganese have repeatedly been reported in the sediments deposited during the early stages of development of some lakes of the temperate climatic zone (see Łącka *et al.*, 1998; Borówka and Tomkowiak, 2010). According to Crerar *et al.* (1972), this is a characteristic phenomenon observed in shallow, well-oxygenated, oligotrophic reservoirs where conditions favoured the precipitation of manganese hydroxides in the form of $Mn(OH)_4$. The quite high content of Ca in the form of $CaCO_3$ may be associated with the inflow of groundwater

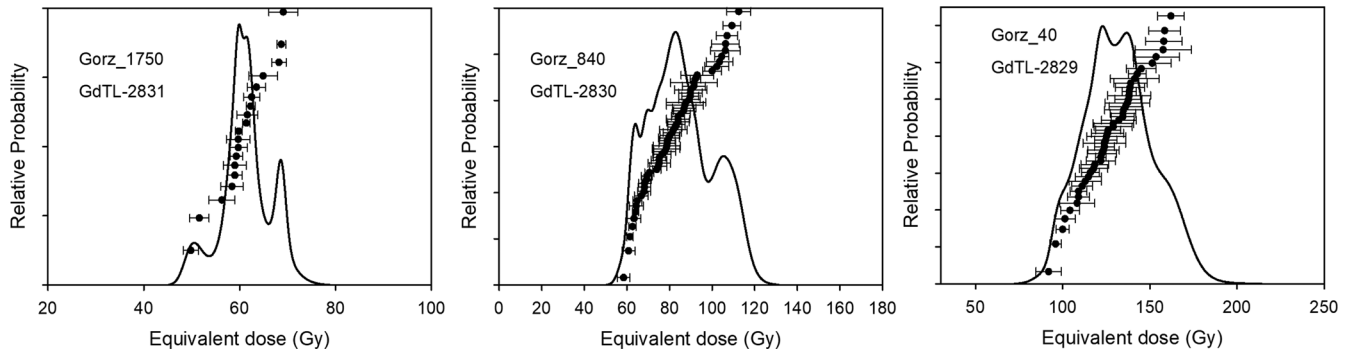

Figure 10. Distributions of obtained equivalent doses as the relative probability density functions (Berger, 2010) for all OSL investigated samples.

Table 5. Distinct phases of the sedimentary basin development at the Gorzów Wielkopolski palaeolakes research area.

Phases of the sedimentary basin development	Lithology		Geochemistry		L PAZ	L MAZ Bone remains	
	Section GS1	Section GS3	Section GS1	Section GS3	Section GS3	Section GS3	Hydroclimatic conditions
Phase I	LLZ-2 (40.0–41.7 m a.s.l.) Calcareous gyttja – increased content of medium- to fine-grained sand (ca. 10–20%) – increase of Mz from 5.5 at the bottom to 6.5 phi at the top	LLZ-1a (48.6–49.2 m a.s.l.) Calcareous gyttja – sand fraction recognised – Mz value in the range of 2–6 phi	GLZ-2 (40.0–40.25 m a.s.l.) – low organic matter content and TOC – increased content of lithophilic elements (Na, K, Mg) as well as Fe and Mg GLZ-3 (40.25–41.0 m a.s.l.) – increased content of organic matter, S and Fe – decrease content of Mn	GLZ-1a (48.6-49.2 m a.s.l.) – increased content of K, Fe, Mn, Zn – upward decrease of Fe/Mn and erosion index	L PAZ-1 ***Betula*-NAP** (*Betula nana*, *Juniperus*, *Artemisia*, Poaceae)	M1 Characeae, *Typha* sp., *Ceratophyllum demersum*	Climate typical for park tundra; vast free open space resulting in intensification of mineral matter delivery to the lake basin; onset of permafrost degradation and Ca-rich groundwater influx to the lake. Increase of lake water level and growth of redox conditions in southernmost (deeper) part of the lake. **Late Saalian Glaciation/ Early Eemian (MIS 6 / MIS 5e)**
Phase II	LLZ-3 - LLZ-6 (41.0–50.6 m a.s.l.) Calcareous gyttja – in the lower part (LLZ-3 & 4) initially increase of clay and decrease of silt fraction – above (LLZ-5 & 6) increase of sand content and decrease of clay and silt fraction – decrease of Mz and increase of SD values	LLZ-1b & 1c (49.2–52.6 m a.s.l.) Calcareous gyttja/ limnic chalk – slight increase of mid- to coarse-grained mud content	GLZ-4 (41.0–50.9 m a.s.l.) - high content of Ca, Mg, Mn and total carbon (TC), – decrease of Fe and S content (GLZ-4a & 4b) – continuous decrease of Mg (GLZ-4c, 4d & 4e) – - increase of potassium content (GLZ-4d & 4e)	GLZ-1b & 1c (49.2–52.6 m a.s.l.) - high content of Ca, Mg, Mn, TC and progressive decrease of Fe content - low content of organic matter, TOC and sulphur	L PAZ-2–LPAZ-7 ***Betula-Pinus*** ***Pinus-Betula-Ulmus*** ***Quercus-Fraxinus-Ulmus*** ***Corylus-Quarcus-Alnus*** ***Corylus-Tilia-Alnus*** ***Carpinus-Corylus-Alnus*** **Deer bone (uppermost part of lacustrine deposits)**	M2–M4 *Najas marina* *Typha* sp. *Nuphar lutea*, *Nyphaea alba*, *Brasenia* sp., *Trapa natans*, *Betula*, *Pinus*, *Alnus*, *Tilia*, *Carpinus*, *Corylus*, *Juniperus*, *Picea* **Rhinoceros bone remains** **Eemian Interglacial (MIS 5e)**	Succession of plants typical for the Eemian Interglacial. Intensive Ca-rich groundwater inflow to the lake; stepwise shallowing of the lake coinciding with calcareous sediments deposition, with upward increasing allochthonous mineral deposits content.

(*Continued*)

Table 5. (*Continued*)

Phases of the sedimentary basin development	Lithology		Geochemistry		L PAZ	L MAZ Bone remains	
	Section GS1	Section GS3	Section GS1	Section GS3	Section GS3	Section GS3	Hydroclimatic conditions
Phase III	LZZ-7(50.6–51.3 m a.s.l.)Silty sand with organic matter, especially at 50.9 m a.s.l.	LLZ-2(52.6–53.2 m a.s.l.)Peat with sand at the bottom	GLZ-5(50.9–51.3 m a.s.l.)- at the bottom (~50.9 m a.s.l.) higher content of organic matter, TOC, N, S and Fe- residual content of Ca and increase of Na, K, Cu and Zn concentration	GLZ-2(52.6–53.2 m a.s.l.)- high content of organic matter, C, N, S and TOC- initially high content of Fe, afterwards decreasing gradually- low content of Ca, Mg, Mn	LPAZ-8***Picea-Abies-Carpinus***Rapid increase of pine pollen percentage, with at the same time decreasing importance of oak, hazel and hornbeam	M5*Betula, Pinus, Alnus,Betula nanaCarex*	Development of a valley bog evolved on the lacustrine sediments under cold climatic conditions, completed with species typical for tundra vegetation. Probable rise of permafrost in the ground and interruption of intensive feeding of the basin by groundwater.**End of Eemian/ EarlyWeichselian (MIS 5d-5a)**
Phase IV	Upper part of the section (51.3–60.0 m a.s.l.) Fine- and medium-grained sand, deltaic	LLZ-3 (53.2–55.4 m a.s.l.) Sand with a changing grain size, intercalated with silt, horizontally laminated	–	GLZ-3 (53.2–55.4 m a.s.l.) – raised content of lithophyte elements – Na, K, Mg, Cu and Zn; visible correlation between their content and a percentage of silt-clay fraction in the deposit – - insignificant content of Ca	LPAZ-9 i 10 ***Pinus* -*Calluna vulgaris* - NAP-*Pinus*** – significant content of NAP (30–50%) – Co-occurrence of tundra species (*Betula nana*) and plants with higher thermal requirements (i.a. *Tilia*) reflects that they accumulated as a secondary deposit	M6 Small amount of plant macrofossils, *Betula nana* at the upper part	Accumulation of mineral deposits, sandy silt and silt in low-flow conditions, formation of delta at the southern margin of the basin. Low groundwater basin recharge and high surface outwash may indicate existence of permafrost in the ground. **Early Weichselian (MIS 4)**

(*Continued*)

Table 5. (*Continued*)

Phases of the sedimentary basin development	Lithology		Geochemistry		L PAZ	L MAZ Bone remains	
	Section GS1	Section GS3	Section GS1	Section GS3	Section GS3	Section GS3	Hydroclimatic conditions
Phase V	–	LLZ-4 (55.4–57.6 m a.s.l.) Calcareous gyttja/ limnic chalk, small amount of sandy silt	–	GLZ-4 (55.4–57.6 m a.s.l.) – high content of Ca, Mg, Fe and Mn, especially at the initial stage (GLZ-4a)	LPAZ-11 i 12 ***Betula* - NAP** ***Pinus-Betula*** Gradually decreasing content of NAP	M7 & M8 At the beginning, numerous *Betula nana* and *Typha* sp. macrofossils (M7), next replaced with freshwater plants macroremains – Characeae, *Najas marina*, *Najas flexilis* (M8)	Reactivation of lacustrine basin intensively fed with Ca-rich groundwater, climatic conditions shift toward optimum **Early MIS 3**
Phase VI	–	LLZ-5 & 6 (57.6-59. m a.s.l.) Highly disintegrated peat with 20 to 80% of organic matter content. Radiocarbon age ~40,661 cal. BP for plant macrofossils (60 m a.s.l.)	–	GLZ-5 i 6 (57.6-59.6 m a.s.l.) – high content of organic matter, C, N, S and TOC, especially at GLZ-5 level and between 58.0 and 59.1 m a.s.l. – high and gradually increasing Na, K, Mg, Cu, and Zn content, which correlates well with increasing values of erosion index – small but important content of Ca and Mn	–	–	Deterioration of shallow mesotrophic lake and valley-type periodically flooded peat grow **Late MIS 3 (Hengelo - Denekamp?)**

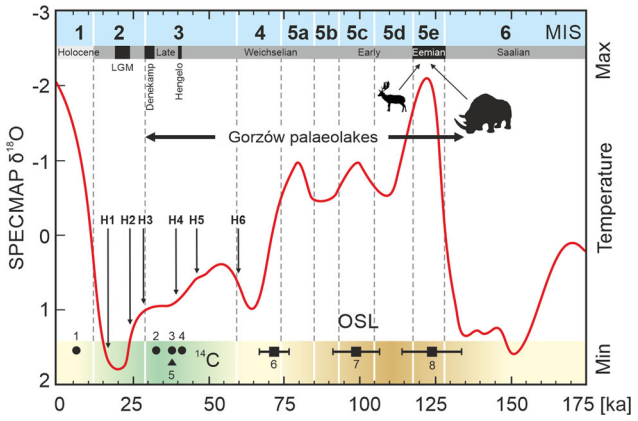

Figure 11. Middle to Late Pleistocene climatic changes based on SPECMAP foraminiferal $\delta^{18}O$ time series (from Winograd *et al.*, 1997) and range of distribution of Gorzów Wielkopolski palaeolakes deposits based on ^{14}C and OSL data, with an indication of Heinrich (H1–H6) glacial-depositional events (from Hemming, 2004). [Color figure can be viewed at wileyonlinelibrary.com].

very rich in $^{-}HCO_3$ and ^{++}Ca ions, derived from the decalcification of glaciofluvial sediments at the bottom of the sedimentation basin. In the initial phase of the reservoir, during the Late Saalian glaciation (MIS 6, GS3-1 L PAZ; Fig. 8), these sediments deposited under cold, dry climatic conditions, when the landscapes were dominated by steppe communities of Poaceae and *Artemisia* and tundras of *Betula nana* and Cyperaceae. They continued accumulating for almost all the Eemian Interglacial (MIS 5e) from E1 (GS3-2 L PAZ) to E5 (GS3-7 L PAZ; Fig. 8), under improving climatic conditions that peaked in the climatic optimum, when varied oak-hornbeam communities dominated forests. The remains of *Stephanorhinus* (Fig. 4F) lay in the upper part of E5 (Fig. 8). The communities of macrophytes spread in the palaeo-reservoir (GS3-M1 to GS3-M4 L MAZs) when the new lake was still relatively deep, reaching approximately 10 m or more, and had transparent waters rich in calcium carbonate. Over time, the lake turned shallow and eutrophied (Fig. 9); five cycles of limnic chalk deposited along its margins, and two in its central part. At the current stage of research, it can only be assumed that this cyclicity is driven by climate. The Ca/Mg and Na/K curves (Fig. 7, S1) show a clear predominance of chemical over mechanical denudation during the accumulation of the lower limnic chalk, although the upper part of both sequences shows a marked decrease in the Na/K ratio. Curves illustrating the variability of the so-called erosion index (Na + K + Mg/Ca) for both exposures show that only during the initial phase were these important processes of sedimentation, and they became negligible later on. This advanced stage of sedimentation correlates with the palaeobotanical samples GS3-8 and GS3-9 L PAZ (E6 and E7, Fig. 8), which correspond to the declining Eemian Interglacial when climatic conditions gradually deteriorated, and boreal pine forests became dominant. The latter is the time that corresponds to level GS3-M5 L MAZ (Fig. 9), which in fact documents a progressive progradation of the lake margins and shallowing and shrinking of the palaeo-reservoir. The last phase of the Eemian lake ended up with the accumulation of the ca. 0.6 m of *D. dama*-bearing peat. In this phase in section GS1, there was an accumulation of ~5 cm of sandy silt containing a significant amount of organic matter. It is worth noting that in both sections GS1 and GS3 the transitional portion between the lower chalk level and the layer of organic sediment is not visible (Fig. 4A), which indicates a fairly rapid change in the water level, as well as in the conditions of sedimentation in the basin. The pollen spectra (GS3-10 L PAZ; Fig. 8) tell us that significant climatic cooling and drying, and thus deforestation, occurred at this time. The area surrounding the lake was then overgrown mainly by heathland, steppe and tundra communities. The absence of a dense plant cover led to an increase in surface flow and redeposition of sediment. The lake shrank, became shallow, and transformed into a peat bog, consistent with the results of the macroremains analysis (GS3-M6 L MAZ, Fig. 9). Silt-sand sediments overlay the lower palaeolake deposits; at the same time sand deposited in the upper part of section GS1. Based on the lithology and structural analysis, this over 10 m thick part of sequence GS1 is interpreted as a delta deposit, or an inflow cone accumulated from the southern side of the sedimentation basin. OSL dating of the sandy inlayer sample of section GS3 gave a central age of 98.9 ± 7.9 ka (MIS5c), which could be correlated with the early phase of Weichselian glaciation (Fig. 11). This result agrees with the palaeobotanical observations which attest to a cold climate and a landscape dominated by specific herbaceous vegetation communities and with the variable spread of woody *Pinus* and *Betula* communities. This horizon, therefore, documents shifting climatic conditions towards colder contexts. This observation correlates with GS3-11 L PAZ, the lower part of GS3-12 L PAZ (Fig. 8), and with GS3-M7 L MAZ (Fig. 9), which also confirms cold climate with tundra vegetation. The upper part of GS3-12 L PAZ (Fig. 8) and level GS3-8m L MAZ (Fig. 9) indicate improved climatic conditions and an increased level of the lake water.

The upper deposits undoubtedly indicate a return of lake sedimentation, as shown by the increase in Ca content (Fig. 7A) to 250–300 mg/g (60–75% $CaCO_3$ calculated). In contrast to the lower limnic chalk, Ca in this layer of carbonate sediment is positively correlated with general sulphur, and negatively with the content of organic matter (LOI), TOC, K, Fe, Cu and Zn (Table 2). This proves that there was a pure chemical precipitation of carbonates, and no contribution by aquatic vegetation. This was most probably associated with the shallowness of the lake, where well-oxygenated waters favoured the precipitation of manganese hydroxides, which was particularly marked at the boundary between the subzones GZ3-4a and 4b. The presence of oxidising conditions is also confirmed by the low Fe/Mn ratio, which persists throughout the period of accumulation of the upper limnic chalk layer (Fig. 7). Moving upwards in sequence GS3 we meet a new set of bog sediments, which are radiocarbon-dated to 40 661 cal yr BP. A thin layer of peat lies directly on the upper limnic chalk, and is covered by a series of glacial sediments; this peat was also dated in section GS4 to about 37.7–32.4 ka cal BP (Table 3). On this basis, it can be assumed that the peat and organic–mineral sediments that rest on the upper limnic chalk accumulated in rather dry and cold climatic conditions shortly before the last ice sheet covered the area of the Polish Lowlands (see Marks *et al.*, 2016). The chemical composition of mineral–organic sediments indicates a significant amount of erosion and mechanical denudation during the filling of the basin. However, chemical denudation processes were not negligible, as evidenced by the reduced, but notable amount of Ca, as well as by the pattern of the curve of the Ca/Mg ratio (Fig. 7). The sedimentary basin had become a periodically flooded swamp. There is a temporal anomaly between the radiocarbon age (41 385–39 928 ka cal BP) of the upper lake sediments and the OSL dating to 72.0 ± 5.2 ka of the overlying glaciofluvial unit. This apparent age inversion between the ^{14}C and OSL dating might be explained by the reworking and redeposition of the quartz grains used for the OSL analysis. In fact, Piotrowski and Sochan (2008, 2009) and Piotrowski *et al.* (2010) reported a radiocarbon age of 34 360 ± 1 500 ka cal BP

(site RAC62 in Fig. 2B) for the peat horizon lying over the gyttja layer that was drilled by cartographic borehole no. 62 (Racław), ca. 5 km north-west of the Gorzów area (Figs 2B and 3). East of the RAC site (Fig. 2B), peats yielded a radiocarbon age > 35.0 ka BP (uncalibrated, open). Finally, glaciofluvial sediments from Łupowo (LUP in Fig.2B) have TL ages ranging from 84.0 ± 12.7 to 79.2 ± 11.9 ka BP (Piotrowski *et al.*, 2010). In the light of the radiometric ages obtained for this study, it can be speculated that a substantial amount of pre-Weichselian quartz grains in the glaciofluvial deposit of section GS3 was reworked during the middle Pleniglacial, with possible only partial quartz bleaching.

During the last stage of evolution of the study area there was the transgression and withdrawal of the Weichselian ice cover towards the area of Pomerania, in the course of a period ranging from about 24 500 to 17 500 years (Rotnicki and Borówka, 1990, 1995a, b; Marks, 2002, 2012; Stroeven *et al.*, 2015). Although the lithology of the sediment that fills the analysed sedimentary basin could suggest that the rock elements were highly susceptible to shear under the stresses imposed by the vertical pressure of ice and by the transgression of an ice sheet that moved relatively fast in this area, no glaciotectonic disturbances were noted. This occurs when the edge of the ice sheet pauses for a long time in one place. After some time, the pressure squeezes the underlying deposits out in front of the margin of the ice sheet (Rotnicki, 1976; Jaroszewski, 1991). Similarly, glacier recession from the Poznań (to the south from the research area) to the Pomeranian (to the north from the research area) phase occurred fairly rapidly in this area. This is consistent with the recent reconstructions of the speed of deglaciation of the European Lowland (Stroeven *et al.*, 2015). The process of glaciation in the study area caused the accumulation of a relatively thick glacial series, which in the GS3 and Racław successions (Fig. 3) exceeded the overall thickness of 10 m. These observations suggest that Gorzów palaeolakes must have survived the Scandinavian ice sheet advance during the Last Glacial Maximum, at the same time preserving Eemian large mammal remains. Following this observation, if we would assume a normal *post mortem* position of the rhinoceros skeleton preceding burial processes, ice sheet overriding fossilised lacustrine sequence could be at least partly responsible for the *S. kirchbergensis* skeleton disarticulation observed on site.

Conclusions

Remains of rhinoceroses of the genus *Stephanorhinus* are known from many European sites, but they generally consist of only a few bones or teeth (Billa and Zervanová, 2015). For this reason, the specimen from Gorzów Wielkopolski is a significant find. Preliminary analyses of this rhinoceros-bearing site indicate that the local sedimentary succession extends throughout a period running from the Eemian Interglacial and Vistulian (Weichselian) glaciation up to the middle Plenivistulian (MIS 5-3). The Gorzów Wielkopolski stratigraphic sequence was the result of a virtually uninterrupted accumulation of siliciclastic and organic sediments from the decline of the Saalian glaciation (MIS 6), through the Eemian Interglacial (MIS 5e) to the Hengelo and Denekamp Interstadials (MIS 3). Sites with similar periods are Hengelo and Moershoofd, in the eastern Netherlands, and Oerel, in Germany (Behre and Lade, 1986; Vandenberghe and Plicht, 2016). Remains of *S. kirchbergensis* had been found at 10 other Polish sites, but most are of unknown age. Polish large mammal fauna are fairly imperfectly known. Most mammal-bearing sites are caves in the Kraków-Częstochowa Upland: Nietoperzowa Cave, Ciemna Cave, Biśnik Cave, Cave in Dziadowa Skała and Deszczowa Cave. Cervids largely dominate the faunal assemblages from these sites, but lists include the brown bear, the cave bear, the cave lion, the grey wolf, the horse *Equus ferus,* the woolly rhinoceros, the woolly mammoth, the aurochs and the steppe bison. Polish mammal-bearing open-air sites include Imbramowice, Jóźwin near Konin and Warsaw-Szczęśliwice, which yielded the remains of four large mammal taxa, i.e. the straight-tusked elephant *Palaeoloxodon antiquus,* the horse *E. ferus,* the woolly rhinoceros and *S. kirchbergensis.* In total there are 17 large mammal species (Kowalski, 1959; Czyżewska, 1962, 1989; Jakubowski et al., 1968; Borsuk-Białynicka and Jakubowski, 1972; Jakubowski, 1988, 1996; Kubiak, 1989a, b; Wojtal, 2007; Stefaniak *et al.*, 2009; Made *et al.*, 2014; Valde-Nowak and Nadachowski, 2014; Stefaniak, 2015; Marciszak *et al.*, 2017). Several species, whose remains have been found at West European interglacial sites (Koenigswald, 1991; Kahlke, 1999; Kolfschoten, 2000; Eissmann 2002; Pushkina, 2007; Musil, 2010), are missing from the Polish fossil record (e.g. *E. hydruntinus*, *Hippopotamus amphibius*, *Bubalus murrensis*). The new site at Gorzów Wielkopolski contributes new knowledge about the interglacial fauna of Poland and Central Europe.

Supporting information

Additional supporting information may be found in the online version of this article at the publisher's web-site.

Acknowledgements. This research was supported by grant 0201/2048/18 'Life and death of extinct rhino (*Stephanorhinus* sp.) from Western Poland: a multiproxy palaeoenvironmental approach' financed by the National Science Centre, Poland. LiDAR DTM data presented in this study were used under academic licences DIO.DFT.DSI.7211.1619.2015_PL_N and DIO.DFT.7211.9874.2015_PL_N awarded to the Faculty of Earth Sciences and the Environmental Management University of Wrocław, in accordance with the Polish legal regulations of the administration of the Head Office of Land Surveying and Cartography. We are also immensely grateful to Paul Mazza for his constructive comments and edits to the early version of this manuscript, which helped us thoroughly improve the text. Finally, we thank Geoffrey Duller for his insightful comments and careful editorial handling. The authors declare no conflicts of interest.

Data availability statement

The data that support the findings of this study are available from the corresponding author upon reasonable request.

References

Aitken MJ. 1998. An introduction to optical dating, *The dating of Quaternary sediments by the use of photon-stimulated luminescence*. Oxford University Press: Oxford.

Alexandrowicz SW, Alexandrowicz WP. 2010. Molluscs of the Eemian Interglacial in Poland. *Annales Societatis Geologorum Poloniae* **80**: 69–87.

Behre K-E, Lade U. 1986. Eine Folge von Eem und 4 Weichsel-Interstadialen in Oerel/Niedersachsen und ihr Vegetationsablauf. *Eiszeitalter und Gegenwart* **36**: 11–36.

Berger GW. 2010. An alternate form of probability-distribution plot for De values. *Ancient TL* **28**: 11–22.

Berglund BE, Ralska-Jasiewiczowa M. 1986. Pollen analysis and pollen diagrams. In *Handbook of Holocene Palaeoecology and Palaeohydrology*, Berglund BE, Ralska-Jasiewiczowa M (eds). John Wiley and Sons Ltd: Chichester, NY; 455–484.

Billa EME, Zervanová J. 2015. New Stephanorhinus kirchbergensis (Jäger, 1839) (Mammalia, Rhinocerotidae) in Eurasia – an account. *Addenda to previous work. Gortania, Geologia, Paleontologia, Paletnologia* **36**: 55–68.

Björck S, Noe-Nygaard N, Wolin J *et al*. 2000. Eemian Lake development, hydrology and climate: a multi-stratigraphic study of the Hollerup site in Denmark. *Quaternary Science Reviews* **19**: 509–536.

Blott SJ, Pye K. 2001. Gradistat: a grain size distribution and statistics package for the analysis of unconsolidated sediments. *Earth Surface Processes and Landforms* **26**: 1237–1248.

Borówka RK. 1992. The pattern and magnitude of denudation in intraplateau sedimentary basins during the Late Vistulian and Holocene (in Polish with English summary). *Adam Mickiewicz University Press, Seria Geografia* **54**: 1–177.

Borówka RK, Tomkowiak J. 2010. Skład chemiczny osadów z profilu torfowiska Żabieniec. In *Torfowisko Żabieniec. Warunki naturalne, rozwój i zapis zmian paleoekologicznych w jego osadach* [In Polish] Twardy J, Żurek S, Forysiak J (eds). Bogucki Prace Muzeum Ziemi: Poznań; 163–172.

Borsuk-Białynicka M, Jakubowski G 1972. The skull of Dicerorhinus mercki (Jäger) from Warsaw. [In Polish] *Prace Muzeum Ziemi* 20: 187–199.

Bos AAJ, Bohncke SJP, Kasse C *et al*. 2001. Vegetation and climate during the Weichselian Early Glacial and Pleniglacial in the Niederlausitz, eastern Germany – macrofossil and pollen evidence. *Journal of Quaternary Science* **16**: 269–289.

Boyle JF. 2001. Inorganic geochemical methods in palaeolimnology. In *Tracking environmental change using lake sediments vol. 2: Physical and geochemical methods*, Last WM, Smol JP (eds). Springer: Dordrecht; 83–141.

Börner A, Hrynowiecka A, Stachowicz-Rybka R *et al*. 2018. Palaeoecological investigations and 230Th/U dating of the Eemian Interglacial peat sequence from Neubrandenburg-Hinterste Mühle (Mecklenburg-Western Pomerania, NE Germany). *Quaternary International* **467**: 62–78.

Bøtter-Jensen L, Bulur E, Duller GAT *et al*. 2000. Advances in luminescence instrument systems. *Radiation Measurements* **32**: 523–528.

Brose F, Luckert J, Müller H *et al*. 2006. Das Eem von Vevais – ein bedeutendes Geotop in Ostbrandenburg [The Eemian of Vevais – an important geotope of the Eastern Brandenburg area]. *Brandenburgische geowissenschaftliche Beiträge* **13**(1/2): 155–164.

Bruj M, Roman M. 2007. The Eemian lakeland extent in Poland versus stratigraphical position of the Middle Polish Glaciations [In Polish]. *Biuletyn PIG-PIB* **425**: 27–34.

Cappers RTJ, Bekker RM, Jans JEA. 2006. Digital seed atlas of the Netherlands. Groningen, Barkhuis/Groningen University Library.

Crerar DA, Cormick RK, Barnes HL. 1972. Organic control on the organic geochemistry of manganese. *Acta Mineralogica-Petrographica* **20**: 217–226.

Czyżewska T. 1962. Upper dentition of Dicerorhinus mercki (Jäger) from Szczęśliwice near Warszawa, Poland. [In Polish] *Acta Palaeontologica Polonica* 7(1–2): 223–234.

Czyżewska T. 1989. Parzystokopytne – Artiodactyla. In *Historia i ewolucja lądowej fauny Polski* [In Polish] Kowalski K. (ed) Folia Quaternaria 59–60: 209–217.

Di Stefano G. 1996. Identification of fallow deer remains on the basis of its skeletal features: taxonomical considerations. *Bollettino della Società Paleontologica Italiana* **34**: 323–331.

Driesch A, von den. 1976. A guide to the measurement of animal bones from archaeological sites. Peabody Museum Bulletin **1**: 1–136.

Eissmann L. 2002. Quaternary geology of eastern Germany (Saxony, Saxon–Anhalt, South Brandenburg, Thüringia), type area of the Elsterian and Saalian Stages in Europe. *Quaternary Science Reviews* **21**: 1275–1346.

Erdtman G. 1960. The acetolysis method. *Svensk Botanisk Tidskrift* **54**: 561–564.

Folk R, Ward W. 1957. Brazos River bar: a study in significance of grain size parameters. *Journal of Sedimentary Petrology* **27**: 3–26.

Galbraith RF, Roberts RG, Laslett GM *et al*. 1999. Optical dating of single and multiple grains of quartz from Jinminum Rock Shelter, Northern 12 Australia. Part I, experimental design and statistical models. *Archaeometry* **41**: 1835–1857.

Gaudzinski-Windheuser S, Kindler L, Pop E *et al*. 2014. The Eemian Interglacial lake-landscape at Neumark-Nord (Germany) and its potential for our knowledge of hominin subsistence strategies. *Quaternary International* **331**: 3–38.

Gromova V. 1935. On the remnants of rhinoceros Merck (*Rhinoceros mercki* Jaeg.) from the Lower Volga. *Trudy PIN RAN* **4**: 91–136.

Gromova V. 1960. Determination key to mammals of USSR based on postracianl bones. [In Russian.] Izdatel'stvo Akademii Nauk SSSR, Moscow.

Guérin C. 1980. Les Rhinoceros (Mammalia, Perissodactyla) du Miocene terminal au Pleistocene superieur en Europe Occidentale. Comparison avec le especes actuelles. *Documents du Laboratoire de Geologie de la Faculte des Sciences de Lyon* **79**: 423–783.

Guérin G, Mercier N, Adamiec G. 2011. Dose-rate conversion factors: update. *Ancient TL* **29**: 5–8.

Hammer Ø, Harper DAT, Ryan PD. 2001. Past: Paleontological Statistics Software Package for Education and Data Analysis. *Palaeontologia Electronica* **4**: 1–9.

Hemming SR. 2004. Heinrich events: massive late Pleistocene detritus layers of the North Atlantic and their global climate imprint. *Review of Geophysics* **42**: 235–273.

Hermsdorf N, Strahl J. 2008. Karte der Eem–Vorkommen des Landes Brandenburg. *Brandenburgische Geowissenschaftliche Beiträge* **15**: 23–55.

Jacobs Z. 2004. *Development of luminescence techniques for dating Middle Stone Age sites in South Africa*. Unpublished PhD thesis, University of Wales, Aberystwyth.

Jakubowski G. 1988. Finding of forest elephant – *Palaeoloxodon antiquus* (Falconer & Cautley, 1847) in Upper Pleistocene deposits of outcrop, Jóźwin of Brown Coal Mine "Konin". [In Polish] *Zeszyty Muzealne* 2: 13–87.

Jakubowski G. 1996. Forest elephant Palaeoloxodon antiquus (Falconer and Cautley, 1847) from Poland. [In Polish] *Prace Muzeum Ziemi* 43: 85–109.

Jaroszewski W. 1991. Rozważania geologiczno-strukturalne nad genezą deformacji glacitektonicznych. [In Polish] *Annales Sosietatis Geologorum Poloniae* 61: 153–206.

Jakubowski G, Krysiak K, Roskosz T. 1968. The Forest elephant Palaeoloxodon antiquus (Falc. & Caut., 1847) from Warsaw. *Prace Muzeum Ziemi* 12, 187-215.

Juggins S 2007. C2: Software for ecological and palaeoecological data analysis and visualisation. User guide Version 1.5. www.staff.ncl.ac.uk/stephen.juggins/C2.pdf

Kahlke RD. 1999. The history of the origin, evolution and dispersal of the late Pleistocene *Mammuthus – Coleodonta* faunal complex in Eurasia (large mammals). Rapid Fenske Companies, Rapid City, SD. 53–55, 1–219.

Karasiewicz TM. 2019. The kettle-hole mire as archives of postglacial changes in biogenic sedimentation (Tuchola Forest, north-Central Poland). *Catena* **176**: 26–44.

Kittel P, Płóciennik M, Borówka RK *et al*. 2016. Early Holocene hydrology and environments of the Ner River (Poland). *Quaternary Research* **85**: 187–203.

Koenigswald von W. 1991. Exoten in der Großsäuger-Fauna des letzten Interglacials von Mitteleuropa. *Eiszeitalter und Gegenwart* **41**: 70–84.

Kolfschoten, van Th. 2000. The Eemian mammal fauna of central Europe. Geologie en Mijnbouw. *Netherlands Journal of Geosciences* **79**: 269–81.

Kowalski K. 1959. A Catalogue of the Pleistocene Mammals of Poland. [In Polish] PWN. Warszawa-Wrocław.

Kozarski S, Nowaczyk B, Tobolski K. 1980. Results of studies of deposits from Stare Kurowo near Drezdenko assigned to the Brørup Interstadial. [In Polish] *Przegląd Geologiczny* 28: 210–214.

Kubiak H. 1989a. Perissodactyla. In *History and evolution of the terrestial fauna of Poland* [In Polish] Kowalski K (ed)., Folia Quaternaria **59–60**: 197–201.

Kubiak H. 1989b. Trąbowce – Proboscidea. In *History and evolution of the terrestial fauna of Poland* [In Polish] Kowalski K (ed)., Folia Quaternaria **59–60**: 203–208.

Kuszell T, Malkiewicz M. 1999. Palynological profiles of the Eemian and Early Vistulian in south-western Poland. *Acta Palaeobotanica* **Supplement 2**: 487–490.

Lister AM. 1996. The morphological distinction between bones and teeth of Fallow Deer (*Dama dama*) and Red Deer (*Cervus elaphus*). *International Journal of Osteoarchaeology* **6**: 119–143.

Lorek I. 1988. The *Dicerorhinus kierchbergensis* (Jäger, 1839) remains from Eemian sediments of Coalmine Konin (Strip Mine Jóźwin) [In Polish] *Zeszyty Muzealne* **2**: 105–112.

Ławacz W, Planter M, Stasiak K *et al.* 1978. The past, present and future of Tyree Mazurian Lakes. *Polish Archives of Hydrobiology* **25**: 233–238.

Łącka B, Starnawska E, Kuźniarski M. 1998. Mineralogy and geochemistry of the Younger Dryas sediments from Lake Gościąż. In Lake Gościąż, Central Poland. A monographic study Ralska-Jasiewiczowa M, Goslar T, Madeyska T, et al. (eds), Kraków: 124–128.

Mackereth FJK. 1966. Some chemical observations on postglacial lake sediments. *The Philosophical Transactions of the Royal Society of London, Series B, Biological Sciences* **250**(765): 165–213.

Made J van der. 2010. The rhinos from the Middle Pleistocene of Neumark-Nord (Saxony-Anhalt). In *Neumark Nord - Ein interglaziales Ökosystem des mittelpaläolithischen Menschen* Mania D (ed.) Veröffentlichungen des Landesamtes für Archäologie - Landesmuseum für Vorgeschichte Sachsen-Anhalt: 333–500.

Made J, van der, Stefaniak K, Marciszak A. 2014. The Polish fossil record of the wolf *Canis* and deer *Alces*, *Capreolus*, *Megaloceros*, *Dama* and *Cervus* in an evolutionary perspective. *Quaternary International* **326–327**: 406–430.

Marciszak A, Kotowski A, Przybylski B *et al.* 2017. Large mammals from historical collections of open-air sites of Silesia (southern Poland) with special reference to carnivores and rhinoceros. *Historical Biology* **31**: 696730.

Marks L. 2002. Last Glacial Maximum in Poland. *Quaternary Science Reviews* **21**: 103–110.

Marks L. 2012. Timing of the Late Vistulian (Weichselian) glacial phases in Poland. *Quaternary Science Reviews* **44**: 81–88.

Marks L, Dzierżek J, Janiszewski R *et al.* 2016. Quaternary stratigraphy and palaeogeography of Poland. *Acta Geologica Polonica* **66**: 403–427.

Mendyk Ł, Markiewicz M, Bednarek R *et al.* 2016. Environmental changes of a shallow kettle Lake catchment in a Young glacial landscape (Sumowskie Lake catchment). North-Central Poland. *Quaternary International* **418**: 116–131.

Mirosław-Grabowska J. 2008. Reconstruction of lake evolution at Rzecino (NW Poland) during the Eemian Interglacial and Early Vistulian on the basis of stable isotope analysis. *Annual Report of the Polish Academy of Science* 90–92.

Mol J. 1997. Fluvial response to Weichselian climate changes in the Niederlausitz (Germany). *Journal of Quaternary Science* **12**: 43–60.

Murray AS, Wintle AG. 2000. Luminescence dating of quartz using an improved single aliquot regenerative-dose protocol. *Radiation Measurements* **32**: 57–73.

Musil R. 2010. The environment of the Middle Palaeolithic sites in Central and Eastern Europe. In *Middle Palaeolithic Human Activity and Palaeoecology: New Discoveries and Ideas* Burdukiewicz JM, Wiśniewski A (eds), Acta Universitatis Wratislaviensis 3207, *Studia Archeologiczne* 41: 121–179.

Naeher S, Gilli A, North RP *et al.* 2013. Tracing bottom water oxygenation with sedimentary Mn/Fe ratios in Lake Zurich, Switzerland. *Chemical Geology* **352**: 125–133.

Nalepka D, Walanus A. 2003. Data processing in pollen analysis. *Acta Palaeobotanica* **43**: 125–134.

Niska M, Mirosław-Grabowska J. 2015. Eemian environmental changes recorded in lake deposits from Rzecino (NW Poland): Cladocera, isotopic and selected geochemical data. *Journal of Paleolimnology* **53**: 89–105.

Noryśkiewicz B. 1978. The Eemian Interglacial at Nakło on the River Noteć (N Poland). *Acta Palaeobotanica* **19**: 67–112.

Pawłowski D, Borówka RK, Kowalewski GA *et al.* 2016. Late Weichselian and Holocene record of paleoenvironmental changes in a small river valley in Central Poland. *Quaternary Science Reviews* **135**: 24–40.

Piotrowski A, Sochan A. 2008. Objaśnienia do Szczegółowej Mapy Geologicznej Polski w skali 1:50 000, ark. Gorzów Wielkopolski. PIG Warszawa.

Piotrowski A, Sochan A. 2009. Szczegółowa Mapa Geologiczna Polski w skali 1:50 000, ark. Gorzów Wielkopolski. PIG Warszawa.

Piotrowski A, Krupiński K, Krzymińska J. 2010. Organic deposits of Eemian Interglacial in Racław in Gorzów Wielkopolski district [In Polish] In Budowa geologiczna, geologia naftowa, wody geotermalne i ochrona środowiska bloku Gorzowa – Pojezierza Myśliborskiego Karnkowski P, Piotrowski A (eds), 80 Zjazd Naukowy Polskiego Towarzystwa Geologicznego, Szczecin 11–14 września 2010 r, pp. 37–41.

Prescott JR, Stephan LG. 1982. The contribution of cosmic radiation to the environmental dose for thermoluminescence dating. Latitude, altitude and depth dependencies. *TLS II* **1**: 16–25.

Pushkina D. 2007. The Pleistocene easternmost distribution in Eurasia of the species associated with the Eemian *Palaeoloxodon antiquus* assemblage. *Mammalian Review* **37**: 224–245.

Rees-Jones J. 1995. Optical dating of young sediments using fine-grain quartz. *Ancient TL* **13**: 9–14.

Reimer PJ, Bard E, Bayliss A *et al.* 2013. IntCal13 and Marine13 radiocarbon age calibration curves 0–50,000 years cal BP. *Radiocarbon* **55**: 1869–1887.

Rother H, Lorenz S, Börner A *et al.* 2019. The terrestrial Eemian to late Weichselian sediment record at Beckentin (NE Germany): First results from lithostratigraphic, palynological and geochronological analyses. *Quaternary International* **501**: 90–108.

Rotnicki K. 1976. The theoretical basis for a model of the origin of glaciotectonic deformations. *Quaestiones Geographicae* **3**: 103–139.

Rotnicki K, Borówka RK. 1990. New data on the age of the maximum advance of the Vistulian ice sheet during the Leszno Phase. *Quaternary Studies in Poland* **9**: 73–83.

Rotnicki K, Borówka RK. 1995a. The last cold period in the Gardno-Łeba coastal Plain. *Journal of Coastal Research* **22**(Special Issue): 225–229.

Rotnicki K, Borówka RK. 1995b. Dating of the upper pleni-Vistulian Scandinavian ice sheet in the Polish Baltic middle coast. *Prace PIG* **149**: 84–89.

Rychel J, Karasiewicz MT, Krześlak I *et al.* 2014. Paleogeography of the environment in North-eastern Poland recorded in an Eemian sedimentary basin, based on the example of the Jałówka site. *Quaternary International* **328-329**: 60–73.

Sirocko F, Seelos K, Schaber K *et al.* 2005. A late Eemian aridity pulse in central Europe during the last glacial inception. *Nature* **436**: 833–836.

Shpansky AV. 2016. New finds of Merck rhinoceros (*Stephanorhinus kirchbergensis* Jäger 1839) (Rhinocerotidae, Mammalia) in Ob area Tomsk region. *Geosphere Research* **1**: 24–39.

Skompski S. 1980. Nowe stanowiska mięczaków z osadów interglacjalnych w zachodniej Polsce. [In Polish] *Biuletyn Instytutu Geologicznego* **322**: 5–29.

Stark P, Firbas F, Overbeck F. 1932. Die Vegetationsentwicklung des Interglazials von Rinnersdorf in der ostlichen Mark Brandenburg. *Abhandlungen des Naturwissenschaftlichen Vereins zu Bremen* **28**: 105–130.

Stefaniak K. 2015. *Neogene and Quaternary Cervidae from Poland*. Institute of Systematics and Evolution of Animals, Polish Academy of Sciences. Kraków.

Stefaniak K, Socha P, Nadachowski A *et al.* 2009. Palaeontological studies in the Częstochowa Upland. In *Karst of the Częstochowa Upland and of the Eastern Sudetes: palaeoenvironments and protection*, Stefaniak K, Tyc A, Socha P (eds). Studies of the Faculty of Earth Sciences, University of Silesia: Sosnowiec-Wrocław; 85–144.

Stockmar J. 1971. Tablets with spores used in absolute pollen analysis. *Pollen et Spores* **13**: 615–621.

Straszewska K, Stupnicka E. 1979. Sites of the Quaternary lacustrine and peaty deposits in Poland. *Bulletin of the Polish Academy of Sciences* **27**: 169–177.

Stroeven AP, Hättestrand C, Kleman J *et al.* 2015. Deglaciation of Fennoscandia. *Quaternary Science Reviews* **147**: 91–121.

Tudyka K, Miłosz S, Adamiec G *et al.* 2018. μDose: A compact system for environmental radioactivity and dose rate measurement. *Radiation Measurements* **118**: 8–13.

Urbański K, Winter H. 2005. The Eemian Interglacial in the section Radówek (Łagów lakeland, western Poland) and its implication for till lithostratigraphy. [In Polish with English summary]. *Przegląd Geologiczny* **53**: 418–424.

Valde-Nowak P, Nadachowski A. 2014. Micoquian assemblage and environmental conditions for the Neanderthals in Obłazowa Cave, Western Carpathians, Poland. *Quaternary International* **326–327**: 146–156.

Vandenberghe J, van der Plicht J. 2016. The age of the Hengelo interstadial revisited. *Quaternary Geochronology* **32**: 21–28.

Velichkevich F YU, Zastawniak E. 2006. *Atlas of Pleistocene vascular plant macroremains of Central and Eastern Europe, Part I – Pteridophytes and monocotyledons*. Szafer Institute of Botany, Polish Academy of Sciences, Cracow.

Velichkevich FYU, Zastawniak E. 2008. *Atlas of vascular plant macroremains from the Pleistocene of central and eastern Europe, Part II – Herbaceous dicotyledons*. Szafer Institute of Botany, Polish Academy of Sciences: Cracow.

Winograd IJ, Landwehr JM, Ludwig KR *et al*. 1997. Duration and structure of the past four interglaciations. *Quaternary Research* **48**: 141–154.

Winter H, Dobracka E, Ciszek D. 2008. Multiproxy studies of Eemian and early Vistulian sediments at Rzecino site (Łobez Upland, Western Pomerania Lakeland). *Biuletyn Państwowego Instytutu Geologicznego* **428**: 93–110.

Wojtal P. 2007. Zooarchaeological studies of the Late Pleistocene sites in Poland. Institute of Systematics and Evolution of Animals, Polish Academy of Science, Kraków.